# RAY PROPAGATION

# IN

# DIELECTRIC LOADED WAVEGUIDES

---

A Thesis

Presented to

The Faculty of Graduate Studies and Research

The University of Manitoba

---



In Partial Fulfillment

of the Requirements for the Degree

Master of Science in Electrical Engineering

---

by

James Edward Robinson

July 1967

## *ABSTRACT*

*The propagating electric fields in rectangular waveguides loaded by one or several dielectric layers is evaluated using the ray-optical technique. Since this involves the summation of fields on a large number of rays, the alternative technique of the angular spectrum of plane waves is also employed to obtain a continuous sum. The salient features of both methods are presented and the results are compared with reference to accuracy and computational advantages. It is shown that the exact solution can be interpreted in terms of geometrical-optics and diffracted rays which give a better physical insight into the mechanisms of field propagation in dielectric loaded waveguides.*

ACKNOWLEDGMENTS

The author wishes to thank Dr. M.A.K. Hamid of the Electrical Engineering Department who proposed the topic and supervised the research throughout.

Thanks are also due to Dr. A. Wexler for his encouragement and to Miss B.D. Skalenda for her excellent typing of the manuscript.

The use of the computing facilities at the University of Manitoba is also acknowledged.

The financial support of the National Research Council of Canada in the form of an NRC Bursary and a Research Grant (A-3326) is deeply appreciated.

# TABLE OF CONTENTS

# LIST OF FIGURES

# CHAPTER I

# INTRODUCTION

## 1.1 Objectives

Wave propagation in rectangular waveguide loaded by layered dielectric is studied using rays rather than modes. The basic aim of this investigation is to clarify the nature of these waves and to test the validity of a simplified solution using rays. In addition, it is anticipated that the results may be useful in other microwave problems such as loaded horns, loaded guides, filters, phase shifters, etc., or as a useful reference for solving other scattering problems involving layered dielectric[1,2].

## 1.2 Presentation

The basic ray theory is presented in detail in Chapter II. This includes both an asymptotic and an integral formulation of the field of a line source[3,4,5]. The integral formulation of the field as an angular spectrum of plane waves is employed in a limited ray sense to overcome the computational difficulty of the multi-layer case. Scattering of plane and cylindrical waves by plane parallel dielectric layers is also developed. Using these techniques, ray solutions are obtained for the single and multi-layer cases in Chapter III. Finally, the validity and physical interpretations of the ray solution are discussed and related problems are considered.

# CHAPTER II

## BASIC RAY THEORY

### 2.1 Introduction.

The ray method is one of the oldest techniques of science[6]. Greek philosophers Empedocles (490-430 B.C.) and Euclid (300 B.C.) were aware of the geometrical optics ray. Pierre De Fermat (1601-1665) was first to formalize the principle that "Nature always acts in the shortest time". According to his principle light propagation must follow a path of least time between source and receiver. Such paths are known as rays.

The ray technique is often regarded as an alternative approach to the classical boundary value method for solving many field problems. This results from the fact that rays often give a better physical insight into the problem and provide considerable computational advantages.

The ray method is asymptotic[7] and hence the accuracy of the results improves as the wave number K or the distance between source and receiver increases to infinity. A problem is solved after the construction of a ray diagram which shows all the ray paths traced from the source to the receiving point. The resultant field at this point is determined by summing the fields on all the rays, taking into account scattering by all bodies present in the medium.

### 2.2 Ray Amplitude and Phase

The following methods of geometrical optics are usually valid for calculating ray amplitude and phase[3,8,9,10].

The phase is determined by the optical path, i.e.:

$$\phi(S) = \phi_o + \int_o^S K dS \qquad (2.2.1)$$

where the parameters are defined as follows:

| | | |
|---|---|---|
| $\phi(S)$ | - | phase at distance S |
| S | - | distance along the optical path relative to the reference |
| $\phi_o$ | - | reference phase |
| K | - | wave number |

and where the ray path is subject to the usual constraints of Fermat's principle.

The ray amplitude is determined by applying the principle of conservation of energy to a bundle of rays:

$$|A(S)|^2 d\sigma = |A(o)|^2 d\sigma_o \qquad (2.2.2)$$

where amplitudes and areas are defined as:

| | | |
|---|---|---|
| A(o), A(S) | - | complex ray amplitudes at reference and observation points respectively. |
| $d\sigma_o$, $d\sigma$ | - | cross-section of a bundle of rays at reference and observation points respectively. |

Combining equations (2.2.1) and (2.2.2) the equation describing the field on a propagating ray is found to be [3]:

$$A(S) = A(o) \left(\frac{d\sigma_o}{d\sigma}\right)^{1/2} e^{j\phi(S)} \qquad (2.2.3)$$

## 2.3 Field of a Line Source

Rays can be found for any source emitting radiation such as a point source, line source, etc. However, since a line source is used in a later chapter, rays emitted by a line source are now examined[3]. Furthermore, the exact field representation for a line source in free space is reviewed using the concept of angular spectrum of plane waves[4,6].

In this analysis the line source is assumed to be infinitesimally thin and the current intensity is invariant along the axis. Using the magnetic vector potential, the field of the line source is of the form[12]:

$$d\bar{A}_y = dA_y \hat{i}_y = J_y \frac{ds'}{4j} H_o^{(1)}(KR)\hat{i}_y \qquad (2.3.1)$$

and in the radiation zone,

$$\bar{E}_y = -j\omega\mu\bar{A}_y \qquad (2.3.2)$$

or using a common asymptotic representation, (2.3.2) reduces to:

$$E_y \sim -\frac{\omega\mu I_o}{\sqrt{8\pi}} \frac{e^{j(KR-\pi/4)}}{\sqrt{KR}} \qquad (2.3.3.)$$

$\bar{A}$ is defined as the magnetic vector potential and R is the distance from the source to the receiver. Equation (2.3.3) is the well-known asymptotic form of the field due to a line source of strength $I_o$ and is a valid approximation if KR is large (KR>>1). Hence the field of a line source is expressed in terms of the field on a ray.

The field can also be expressed exactly in the integral form[6]:

$$E_y = -\frac{\omega\mu I_o}{4\pi} \int_{-\frac{\pi}{2}+i\infty}^{\frac{\pi}{2}-i\infty} e^{iKR\cos\theta} d\theta \qquad (2.3.4)$$

The above equation is the well-known angular spectrum of plane waves. The integration represents a continuous summation of plane waves over the range $-\pi/2 < \theta < \pi/2$.* Each plane wave field can be interpreted as the field on a ray due to a plane wave source. It will be shown later that the analysis and field summation is greatly simplified if the field on each plane wave in the integrand of (2.3.4) is regarded as the field on a ray.

---

* The path of integration is shown in Figure (2.3.1).

Equation (2.3.4) can be expressed in a more convenient form by relocating the source as shown in Figure (2.3.2).* The resulting field is given by:

$$E_y = \frac{-\omega\mu I_o}{4\pi} \int_{-\frac{\pi}{2}+i\infty}^{\frac{\pi}{2}-i\infty} e^{iK(x\pm x_o)\cos\alpha'} e^{iKZ\sin\alpha'} d\alpha' \qquad (2.3.5)$$

which is the form used in a later chapter.

The field of a line source is presented in the preceding sections in terms of an asymptotic form and an exact integral representation. Hence the radiated field can be expressed in terms of the field on a ray or a continuous sum of plane waves.

## 2.4 Scattering of Line Source Rays by Plane Dielectric Layers

In this section the scattering coefficients for a cylindrical wave incident on one or more dielectric layers, with polarization perpendicular to the plane of incidence, are evaluated. Once these coefficients are known, the scattered field of a line source parallel to plane lossless dielectric layers can be found using the ray method.

J.B. Keller and K.O. Friedericks have considered the problem of a line source parallel to a plane air-dielectric interface[3] as shown in Figure (2.4.1). Scattering coefficients were found by matching fields across the interface such that all boundary conditions were satisfied. This method is now reviewed and extended.

Consider the scalar wave given by $\psi(x,y)$ incident on the dielectric

---

* This form is found by changing $S_1(0,0)$ to $S_2(x_o,0)$ and introducing the new variable $\alpha'$ for the angle $(\theta' + \phi')$. (2.3.5) is more conveniently applied to problems in Chapter III than (2.3.4).

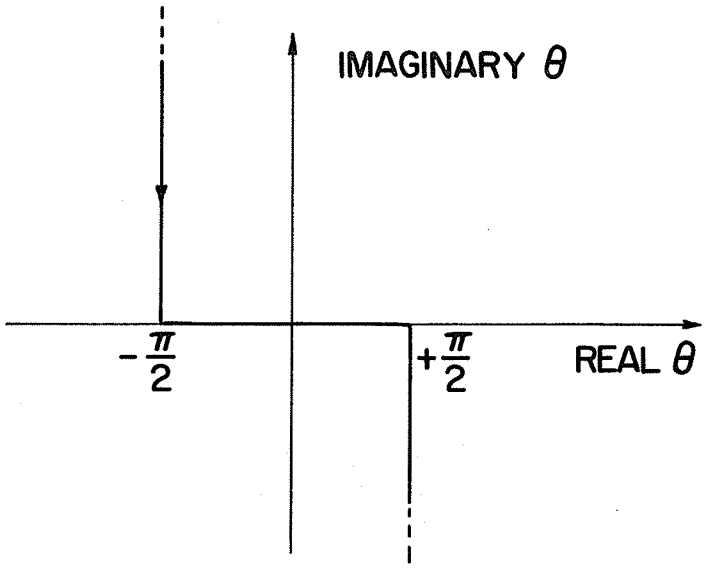


PATH OF INTEGRATION IN THE COMPLEX $\theta$ PLANE FOR THE INTEGRAL IN EQUATION (2.3.4)

FIGURE (2.3.1)

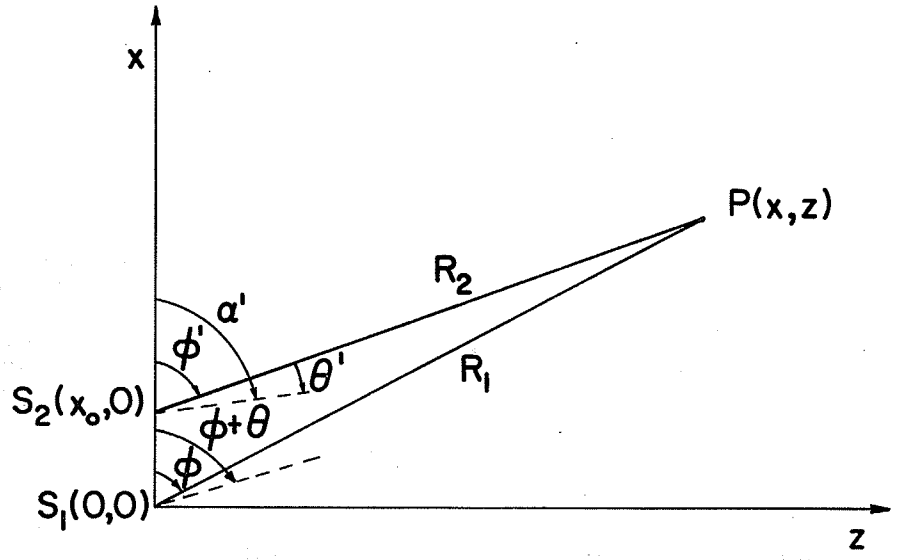


COORDINATES FOR THE RELOCATED PLANE-WAVE SOURCE

FIGURE (2.3.2)

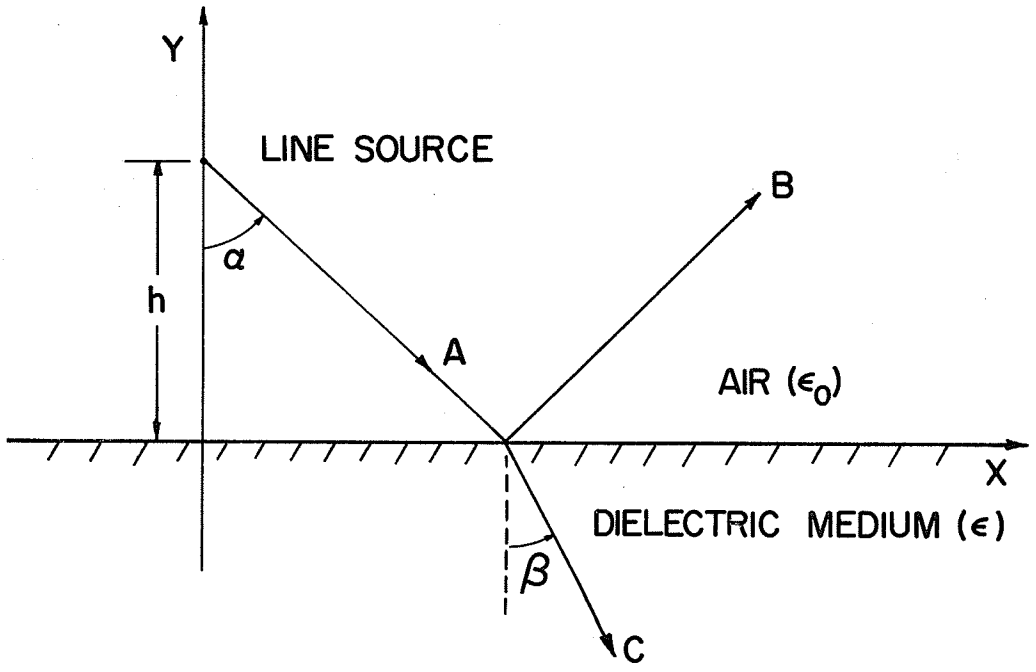


SCHEMATIC DIAGRAM SHOWING THE LINE SOURCE PARALLEL TO AN AIR-DIELECTRIC INTERFACE

FIGURE (2.4.1)

interface of Figure (2.4.1) subject to the following boundary conditions:

$$\psi(x,o^+) = a\psi(x,o^-) \tag{2.4.1}$$

$$\frac{\partial}{\partial_y}\psi(x,o^+) = b\frac{\partial}{\partial_y}\psi(x,o^-) \tag{2.4.2}$$

where

$$\psi \sim A_o \frac{e^{iKR}}{\sqrt{iKR}} + B(x,y)\frac{e^{iKR'}}{\sqrt{iK}}, \quad y>o \tag{2.4.3}$$

$$\sim C(x,y)\frac{e^{iK'\phi}}{\sqrt{iK'}}, \quad y<o \tag{2.4.4}$$

and

$$(R')^2 = x^2 + (y+h)^2 \tag{2.4.5}$$

The results of Keller and Friedericks are given by the following expressions:

$$B(x,y) = A_o \frac{1-V}{1+V}\frac{1}{\sqrt{R'}} \tag{2.4.6}$$

$$C(x,y) = A_o \frac{2}{1+V}\frac{(\sin\alpha)^{1/2}\cos\beta}{a\cos\alpha}$$

$$\cdot \left[|x| - (\mu^{-2}-1)\,h\tan^3\alpha\right]^{-1/2} \tag{2.4.7}$$

$$V = \frac{\mu b\cos\beta}{a\cos\alpha} \tag{2.4.8}$$

$$K' = \mu K \tag{2.4.9}$$

The functions $B(x,y)$ and $C(x,y)$ may be derived using the energy conservation principle of section (2.2) combined with plane wave scattering coefficients at an air-dielectric interface. For this

problem, tubes of rays are defined by making an incremental analysis of the ray path as shown in Figure (2.4.2). The intensity of the ray field may be easily found once the cross-sections of the tubes of rays and scattering parameters are determined.

Using Figure (2.4.2) and the incremental analysis method, the ray intensity is found as follows:

$$\Delta\ell_1 = h \sec\alpha . \Delta\alpha \tag{2.4.10}$$

$$\Delta\ell_2 = h \sec^2\alpha . \cos\beta . \Delta\alpha \tag{2.4.11}$$

$$\Delta\ell_3 = \{h \sec^2\alpha . \cos\beta + \frac{|y|}{\mu} \sec^2\beta\cos\alpha\} \Delta\alpha \tag{2.4.12}$$

Recalling equation (2.2.3) we have:

$$C(x,y) = \left(\frac{\Delta\ell_2}{\Delta\ell_3}\right)^{1/2} A_o \quad (h \sec\alpha)^{-1/2} \frac{2}{1+V} \tag{2.4.13}$$

Using equations (2.4.11) and (2.4.12) a further simplification is made:

$$C(x,y) = A_o \frac{2}{1+Z} \frac{(\sin\alpha)^{1/2} \cos\beta}{a \cos\alpha}$$

$$\cdot \quad [|x| - (\mu^{-2} - 1) \; h \tan^3\alpha]^{-1/2} \tag{2.4.14}$$

The details of this simplification are given in Appendix A2.2. Equation (2.4.14) is in exact agreement with the form given by Keller and Friedericks (2.4.7).

An extension of the incremental analysis technique to the multi-layer case is shown in Appendix A2.2 and a numerical example is given in Appendix A2.3.

Two important points concerning refraction and reflection of cylindrical waves are now evident. Plane wave reflection and transmission coefficients relate the fields across a dielectric interface as seen in

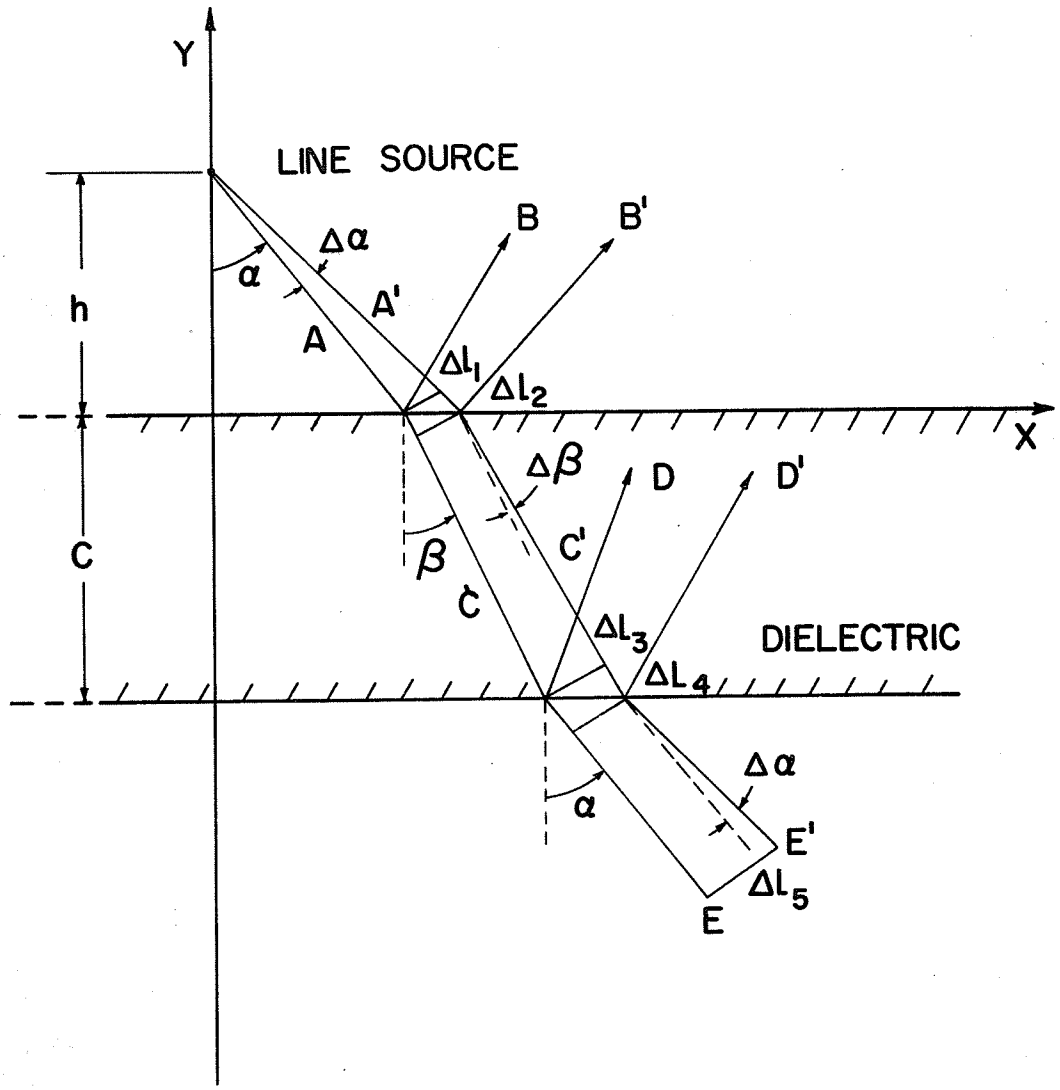


GEOMETRY USED IN THE INCREMENTAL ANALYSIS OF THE SCATTERED RAYS FOR THE PLANE FINITE DIELECTRIC LAYER

FIGURE (2.4.2)

equations (2.4.6) and (2.4.7). Secondly, a doubly refracted cylindrical wave is not cylindrical directly after being doubly refracted. However, the wave approaches a cylindrical wave asymptotically as the distance away from the second interface increases ($K(n+c)>>1$). This ray, E, is shown in Figure (2.4.2) and the field on the ray is developed in Appendix A2.1.

## 2.5. Scattering of Plane Waves by Plane Dielectric Layers

The scattering coefficients of a plane wave incident with polarization perpendicular to the plane of incidence on an air-dielectric interface are well known[6]. Assuming the air as medium 1 and the dielectric as medium 2, the equations may be written in the following form:

$$\frac{E_1}{E_o} = r_1 = \frac{K_1\cos\alpha - K_2\cos\beta}{K_1\cos\alpha + K_2\cos\beta} \qquad (2.5.1)$$

$$\frac{E_2}{E_o} = t_1 = \frac{2K_1\cos\alpha}{K_1\cos\alpha + K_2\cos\beta} \qquad (2.5.2)$$

$$t_1 = 1 - r_1 \qquad (2.5.3)$$

where the parameters are defined as follows:

$E_o$ - incident field (medium 1),

$E_1$ - reflected field (medium 1),

$E_2$ - transmitted field (medium 2),

$\alpha$ - angle of incident wave,

$\beta$ - angle of transmitted wave,

$K_1$ - wave number, medium 1,

$K_2$ - wave number, medium 2.

Similary, a wave travelling from medium 2 to medium 1 has the reflection and transmission coefficients:

$$r_2 = -r_1 \tag{2.5.4}$$

$$t_2 = 1-r_2 \tag{2.5.5}$$

The advantages of the plane wave source are now apparent. Intensity of a scattered plane wave may be found using the relatively simple plane wave reflection and transmission coefficients. In addition, the field on the scattered rays may be easily expressed in closed form using elementary techniques. These advantages are very important for the solution of multiple dielectric layer problems as shown later.

As an example we consider a dielectric plane layer of electrical thickness $\delta$. A plane wave of amplitude $E_o$ is incident on the layer with polarization perpendicular to the plane of incidence. The reflected field can be expressed as an infinite summation of rays:

$$E_1 = E_o \{r_1 + t_1t_2r_2e^{-i2\delta} + t_1t_2r_2^3e^{-i4\delta}+...\} \tag{2.5.6}$$

However, unlike the cylindrical wave case the plane waves can be reduced to a simple form:

$$E = E_o \left[ r_1 + \frac{t_1t_2r_2e^{-i2\delta}}{1-r_2^2e^{-i2\delta}} \right] \tag{2.5.7}$$

## 2.6 Summary

Ray amplitude and phase equations are reviewed. These results are applied to find the scattering coefficients for a line source field in the presence of plane lossless dielectric layers.

The exact field of a line source in terms of the angular spectrum of plane waves is also reviewed. This integral is used to obtain

a closed form solution for the scattered field as a sum of plane wave fields.

# CHAPTER III

## APPLICATION TO DIELECTRIC LOADED WAVEGUIDES

### 3.1 Introduction

Basic ray theory developed in Chapter II is applied to rectangular waveguide transversely loaded with one or more dielectric layers. Simple asymptotic solutions are presented for the single dielectric layer case. The solutions for the multi-layer cases are based on an approximate form of the angular spectrum. Both solutions are compared with the exact solution and physical interpretations are made.

The numerical examples presented in this chapter correspond to a rectangular waveguide operating in the $LSE_{mo}$ (longtitudinal section electric) mode at a frequency of 10.0 GHZ. The inner dimensions of the waveguide are 2.28 x 1.02 cm. (0.9 x 0.4 inches) while the dimensions of the dielectric material are 0.78 x 1.02 cm. Approximating the physical situation of a short probe inserted vertically into the waveguide, the field is assumed to be excited by a line source parallel to the small dimension and located at an arbitrary position in the transverse plane of the guide[11].

### 3.2 Asymptotic Solution for the Single Layer Case

Since the single layer case is essentially a two-dimensional problem, the ray techniques of Sections (2.3) and (2.4) are directly applicable.

Before the field can be found at the observation point, rays of significant intensity must be traced on a ray diagram. Figure (3.2.1) shows the path of a single ray scattered by a dielectric layer. It is apparent from this figure that the classification of rays is involved.

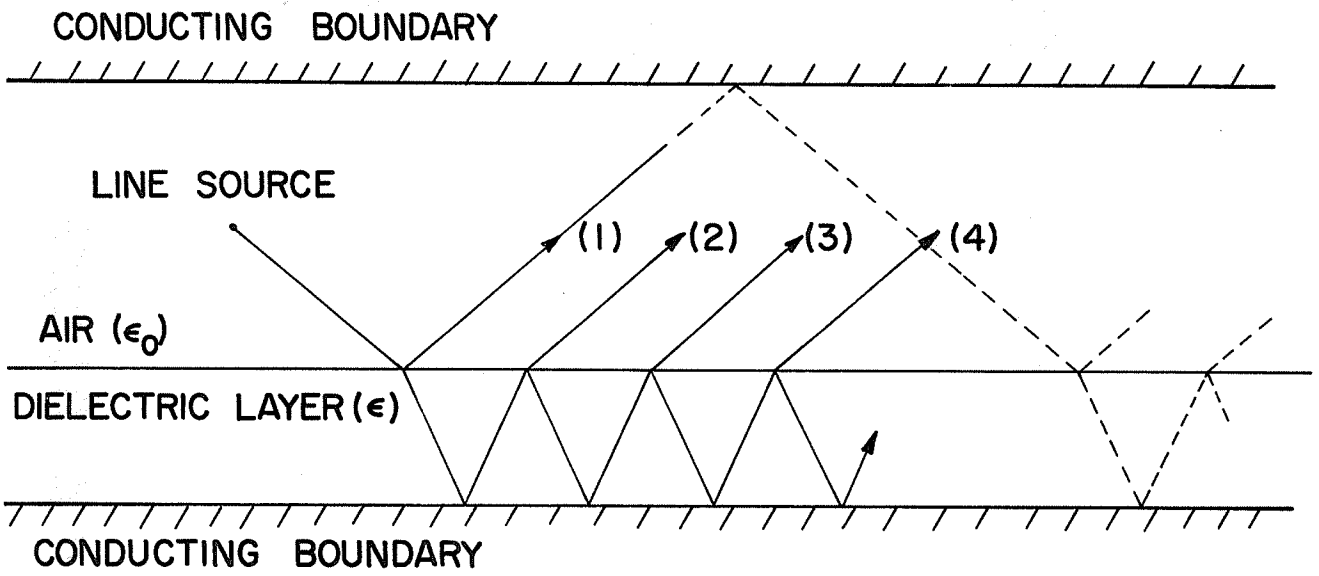


RAY SCATTERING BY THE SINGLE DIELECTRIC LAYER

FIGURE ( 3.2.1 )

Each ray incident on the dielectric layers gives rise to an infinite number of scattered rays as follows:

(1) rays singly reflected;

(2) rays singly transmitted;

(3) rays singly transmitted, internally reflected and re-transmitted; and

(4) rays singly transmitted, internally reflected twice and re-transmitted, etc.

Each of these rays is scattered in the same manner as the incident ray after being reflected at the upper conducting boundary, as shown by the broken lines for the reflected ray, and so on for the higher order rays.

Since the series expression for the ray fields cannot be easily reduced to a closed form expression as in the plane wave case of Section (2.5), an approximate solution is found by retaining only the significant rays. Once these are found the computational problem reduces to the actual summation of a finite number of terms.

For the particular case of a dielectric layer with a relatively small permittivity $\varepsilon$, the significant rays to be considered are: *

(1) the direct ray;

(2) the ray singly reflected at the upper conducting boundary; and

(3) a large number of transmitted rays.

These rays yield the exact solution as $\varepsilon$ approaches $\varepsilon_o$, the free space permittivity, and the distance from the source to the receiver approaches infinity[15].

Reflected rays must be included when $\varepsilon$ is much greater than

---

* The paths of the direct and transmitted rays are shown in Figure (3.2.2).

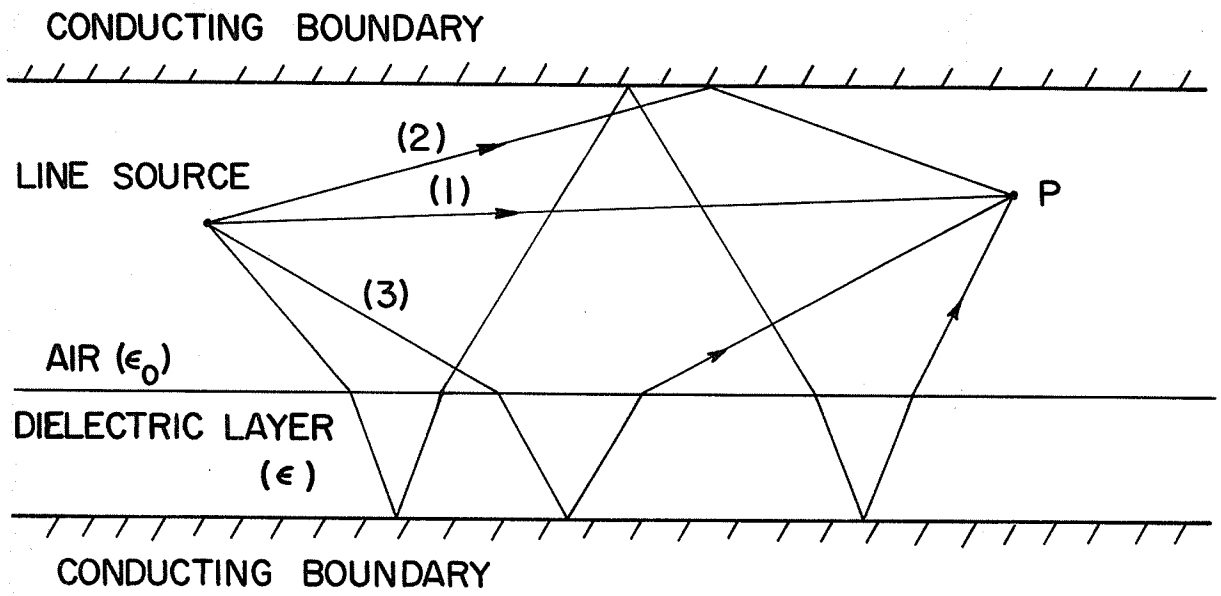


DIRECT AND TRANSMITTED RAY PATHS

FIGURE ( 3.2.2 )

$\varepsilon_o$. This is evident from the expression for the reflection coefficient, i.e.:

$$r = \frac{\cos\alpha - \sqrt{\varepsilon/\varepsilon_o}\cos\beta}{\cos\alpha + \sqrt{\varepsilon/\varepsilon_o}\cos\beta} \qquad (3.2.1)$$

where $\alpha$ and $\beta$ denote the angles of the incident and transmitted rays with respect to the normal, respectively.

The electric field due to types (1) and (2) rays is given by:

$$E_y \sim \frac{-\omega\mu I_o}{\sqrt{8\pi}} \frac{e^{j(KR-\pi/4)}}{\sqrt{KR}} \qquad (3.2.2)$$

while the field on the transmitted rays is given by:

$$E_y \sim \frac{-\omega\mu I_o}{\sqrt{8\pi}} \frac{4V}{(1+V)^2} \left[\Delta x_1 + \frac{\Delta x_2}{\mu} \sec\alpha\right]^{-1/2} \qquad (3.2.3)$$

$$\cdot\ e^{j(KR - \pi/4)}$$

where $\Delta x_1$ and $\Delta x_2$ are defined as follows:

$\Delta x_1$ - total transverse distance along a ray travelling through the unloaded region of permittivity $\varepsilon_o$

$\Delta x_2$ - total transverse distance along a ray travelling through dielectric region of permittivity $\varepsilon$

Appendix A3.1 gives the details of the field summation for a finite number of rays. In addition, it includes a table showing the resultant field at various points across the unloaded section of the guide.

The results of summing types (1), (2), and (3) rays are shown in Figures (3.2.3) and (3.2.4). As seen in these figures, the ray method is a good approximation to the exact solution when $\varepsilon$ is approximately equal

ELECTRIC FIELD IN THE RECTANGULAR GUIDE LOADED BY A SINGLE DIELECTRIC LAYER (I)

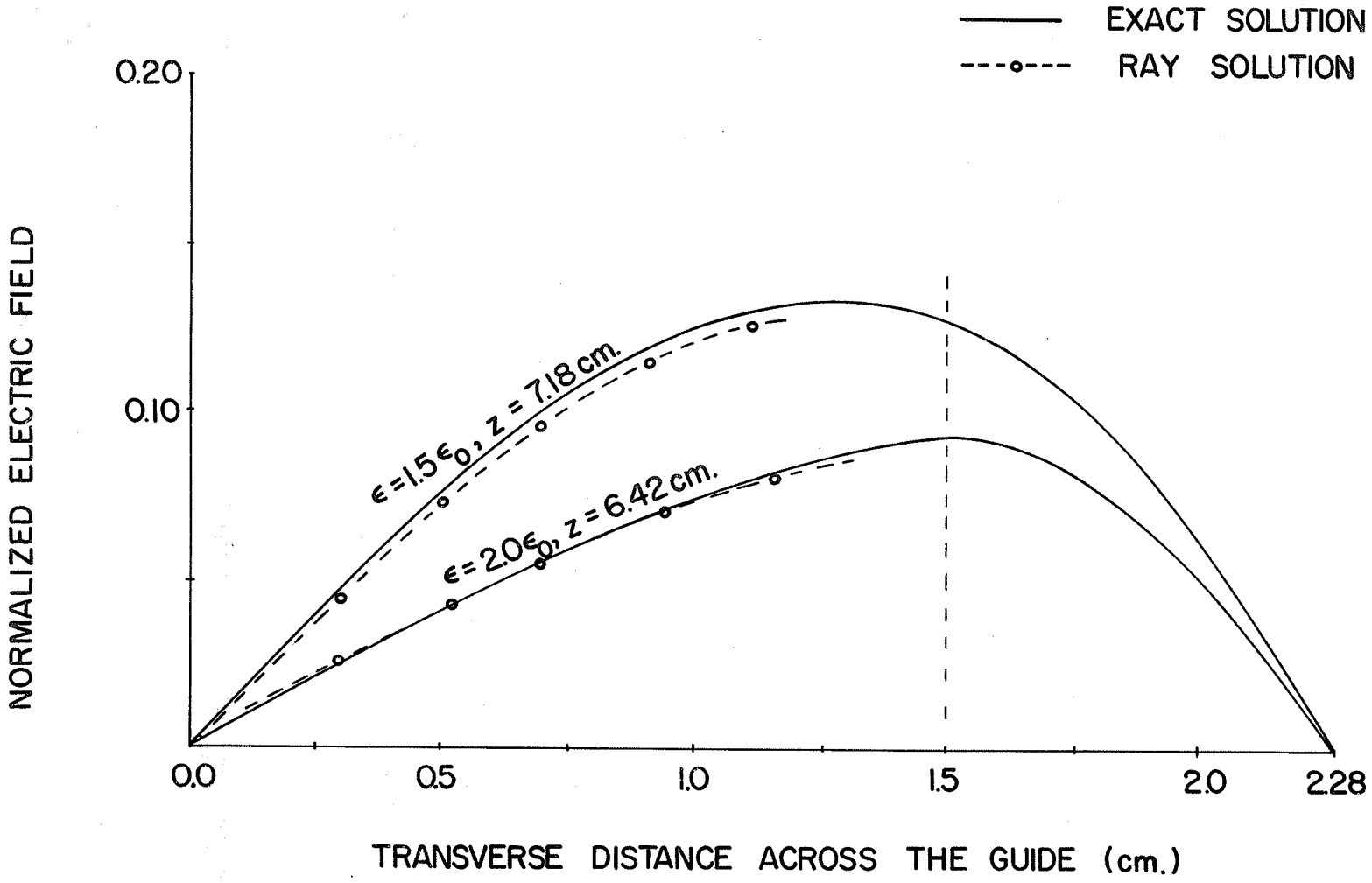


FIGURE (3.2.3)

ELECTRIC FIELD IN THE RECTANGULAR GUIDE LOADED BY A SINGLE DIELECTRIC LAYER (II)

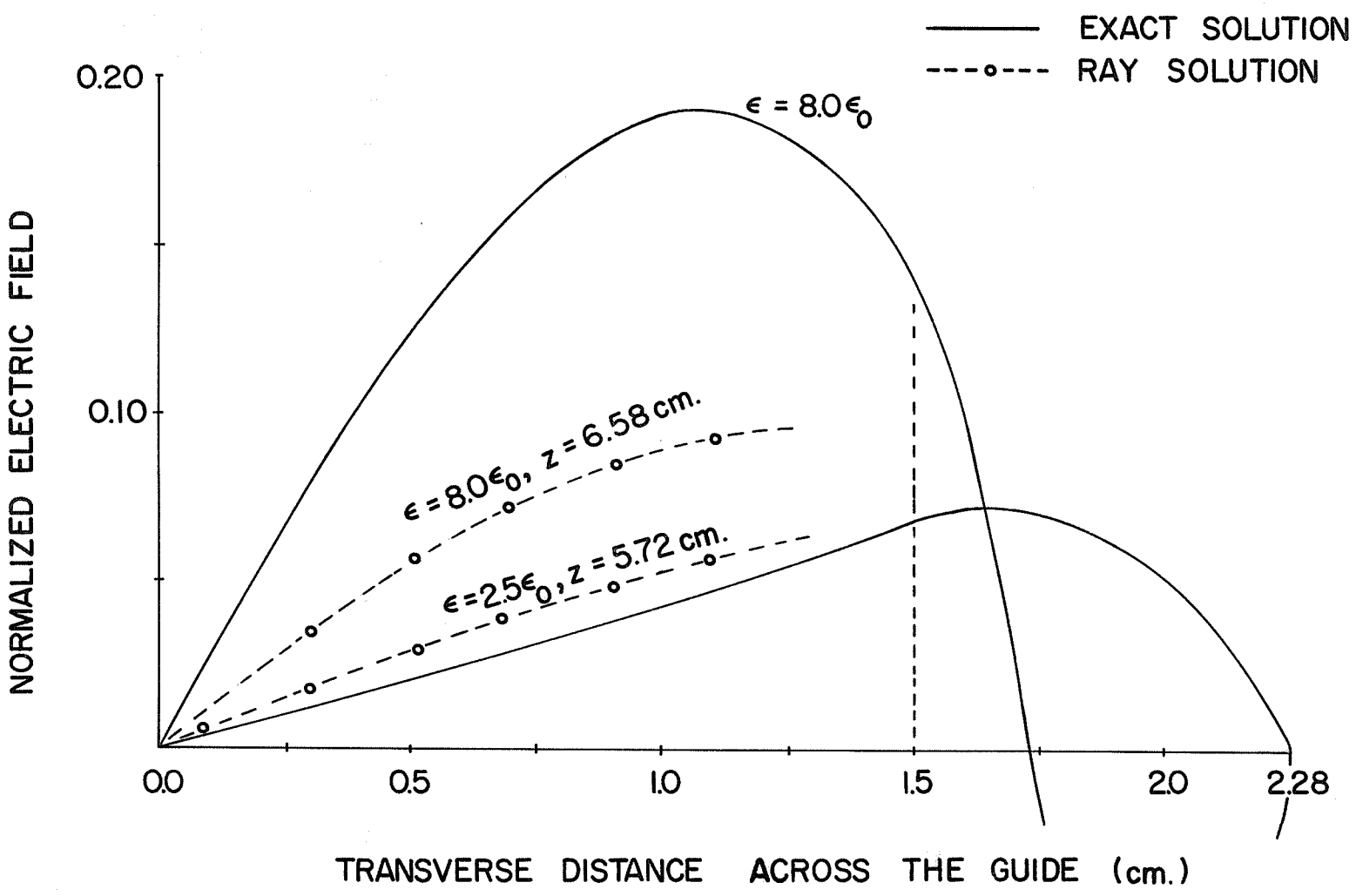


FIGURE ( 3.2.4 )

to $\varepsilon_o$. However, the results shown in Figure (3.2.3) are not in complete agreement with the theory. The case $\varepsilon = 1.5\ \varepsilon_o$, contrary to that expected, is not as accurate as the results for the case $\varepsilon = 2.0\ \varepsilon_o$. However, small errors are to be expected since the solution is asymptotic and an approximate formula is used to calculate the field intensity of the transmitted rays.

The behaviour of the transmitted rays can be inferred from Figures (3.2.3) and (3.2.4). One aspect is evident. As the dielectric permittivity $\varepsilon$ is increased, the cross-section defined by $K_z Z = 4\pi$ is situated closer to the source. $K_z$ is defined as the axial propagation constant and Z is the axial distance between the source and the observer. It follows that the axial propagation constant increases with permittivity $\varepsilon$ (over a limited range) which is due to the increased optical path length of the transmitted rays. In addition, as $\varepsilon$ increases the amplitude of the propagating electric field fluctuates. This can be explained by considering the attenuation of the transmitted rays combined with the constructive and destructive interference between rays as $\varepsilon$ is increased. This explains the increased amplitude of the transmitted field for the case $\varepsilon = 8\varepsilon_o$.

The exact solution used to verify the ray method (Figures (3.2.3) and (3.2.4)) is presented in Section 3.4. $LSE_{mo}$ modes* are assumed to propagate in the loaded waveguide[11,12]. Propagation and amplitude coefficients are found by matching fields across the air-dielectric interface and then applying a well-known integral equation method[11].

Certain disadvantages of the ray method become apparent when the ratio $\varepsilon/\varepsilon_o$ is much greater than unity or if the guide is loaded by multi-layer dielectric. For such cases it is difficult to obtain a simple solution since a large number of rays must be analysed and the fields on these rays summed. This is a basic limitation of problems involving the

---

* Only $LSE_{mo}$ modes propagate since the line source is invariant in the y direction.

propagation of rays through dielectric layers. However, it can be overcome by considering rays from a plane wave source and applying the angular spectrum of plane waves technique.

## 3.3 Angular Spectrum of Plane Waves

The concept of angular spectrum of plane waves is developed by Officer and others[5,13,14] as a continuous summation of rays emitted by a plane wave source. Hence each ray field is treated as a plane-wave rather than a cylindrical wave and the ray fields are summed in an integral rather than as an infinite series. This simplifies the analysis and the summation of ray fields. In addition, either an exact or an approximate solution may be found.

### 3.3.1 Unloaded Rectangular Waveguides

The electric field excited in an empty rectangular waveguide by a line source, parallel to the small dimension, is presented using the angular spectrum of plane waves technique. The field at the observation point, P(x,z) in Figure (3.3.1), can be expressed as the sum of the contributions from the source and its images as a summation of integrals. Each integral is of the form:*

$$E_y = \frac{-\omega\mu I_o}{4\pi} \int_{-\frac{\pi}{2} + i\infty}^{\frac{\pi}{2} - i\infty} [e^{iK(x \pm x_o)\cos\alpha'}][e^{iKZ\sin\alpha'}]d\alpha' \qquad (3.3.1)$$

with the term $e^{iKZ\sin\alpha'}$ common to all integrands. For the positive source and images, the $(x \pm x_o)$ term is defined as follows:

$$(x - x_o) + 2h(\ell) \qquad (3.3.2)$$

$$-(x - x_o) + 2h(\ell+1) \qquad (3.3.3)$$

---

* This is introduced in Section (2.3).

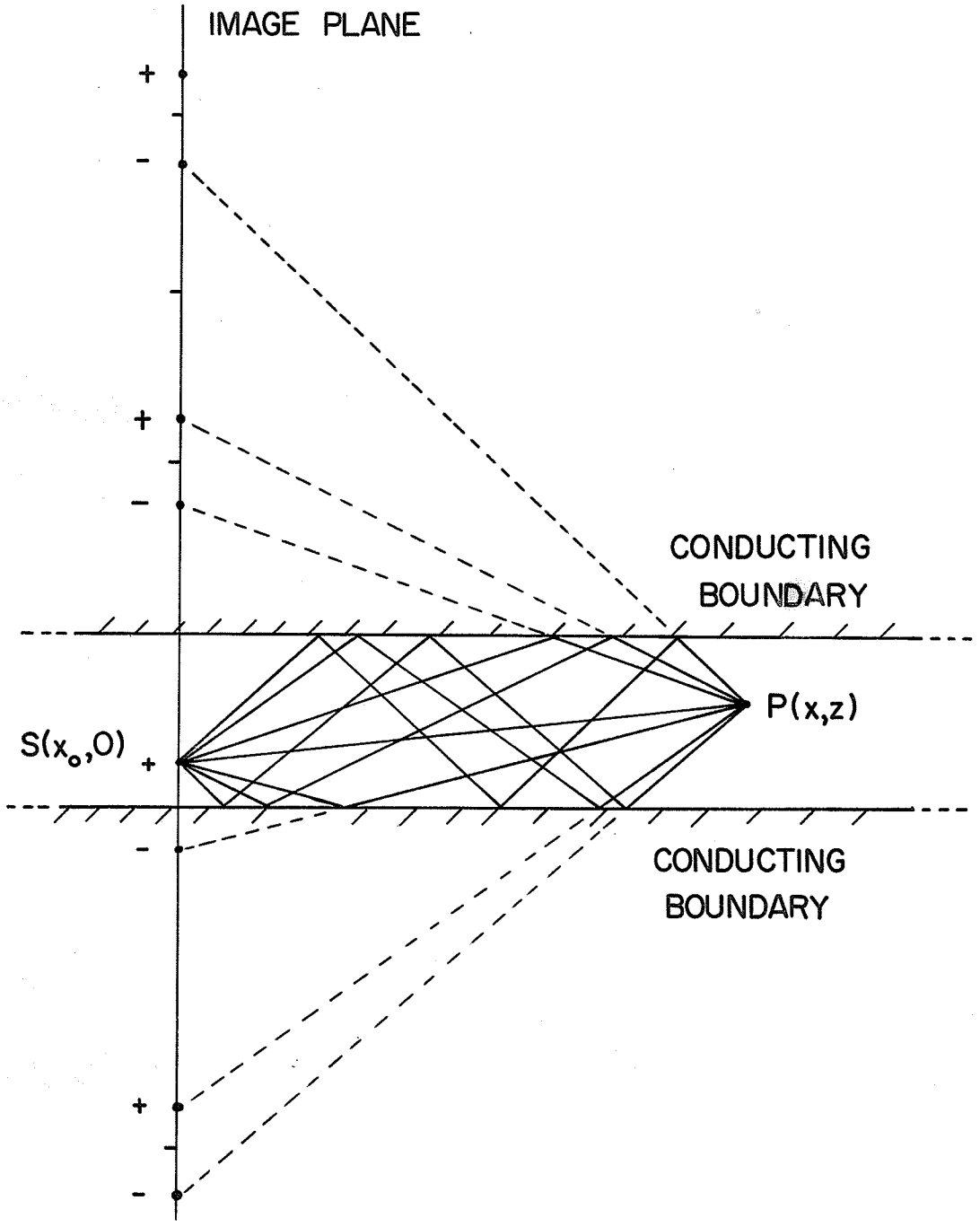


SCHEMATIC DIAGRAM SHOWING THE LINE SOURCE EXCITATION AND IMAGES FOR A RECTANGULAR GUIDE

FIGURE (3.3.1)

$$(x + x_o) + 2h(\ell) \tag{3.3.4}$$

$$-(x + x_o) + 2h(\ell + 1) \tag{3.3.5}$$

where $\ell$ is an integer greater than zero. The contributions due to the source and its images are summed as a single integral, i.e.:

$$E_y = \frac{-\omega\mu I_o}{4\pi} \int_{\frac{-\pi}{2}+i\infty}^{\frac{\pi}{2}-i\infty} \left[ e^{iKZ\sin\alpha'} \right] \left[ \sum_{\ell=o}^{\infty} e^{2bh\ell} \right]$$

$$\cdot \left[ e^{b(x-x_o)} + e^{-b(x-x_o)} + 2bh - e^{b(x+x_o)} + 2bh \right] d\alpha' \tag{3.3.6}$$

where the parameters are defined as:

$$b = iK\cos\alpha', \tag{3.3.7}$$

$$\xi = K\sin\alpha', \tag{3.3.8}$$

$$\xi = K^2 + b^2$$

Equation (3.3.6) is evaluated using contour integration and residue theory. The residue theory is commonly used to evaluate an integral on a closed path in terms of a series expression[16] as follows:

$$\int_C f(Z)dZ = 2\pi i \sum_{m=1}^{\infty} \text{Res } [f(Z)] \tag{3.3.9}$$

For (3.3.6) a pole in the integrand is defined by the condition:*

$$\sinh(bh) = 0 \tag{3.3.11}$$

due to the closed form term of the summation. Hence the solution is found to be:

---

* The summation $[\Sigma\, e^{2bh\ell}]$ in (3.3.6) is a geometric progression and may be reduced to an expression with $[e^{bh} - e^{-bh}]$ in the denominator.

$$\cos \alpha' = \pm \frac{\lambda m}{2h} \tag{3.3.12}$$

and

$$\xi = \left[ K^2 - \left(\frac{\lambda m}{2h}\right)^2 \right]^{1/2} \tag{3.3.13}$$

Applying residue theory, (3.3.6) may be reduced to the well-known form:

$$E_y = \frac{-\omega\mu I_o}{h} \sum_{m=1}^{\infty} \left[ \frac{\sin \frac{m\pi x_o}{h} \sin \frac{m\xi x}{h}}{\xi} \right] e^{j\xi Z} \tag{3.3.14}$$

The advantage of this technique is now apparent. The contributions from the source and images are summed in the same manner as the plane waves in Section (2.5) and are reduced to a simple closed form expression.

### 3.3.2 Rectangular Waveguide Loaded by a Single Dielectric Layer

In order to obtain a simple approximate solution for the waveguide loaded with a single dielectric layer, Officer's work is first reviewed and then extended to the more general case of N layers. An explanation for surface waves along the air-dielectric interface is found using diffracted rays. In addition, cases not involving surface wave propagation are found to be solvable using an approximate ray method, that is, by considering only the dominant rays.

As previously done, the fields on the rays must be summed at the observation point. Since the rays are emitted by a line source, the scattered field due to a ray incident on the dielectric layer is of the form:

$$e^{-b_1(x-d)}\left[1 + e^{-2b_1(H-x)}\left\{r_1 - t_1t_2e^{-2b_2h} + r_2t_1t_2e^{-4b_2h} - r_2^2t_1t_2e^{-6b_2h} + \ldots\right\}\right] \tag{3.3.15}$$

where parameters are defined as:

$$b_1 = iK \cos \alpha_1' \qquad (3.3.16)$$

$$b_2 = iK\sqrt{\epsilon/\epsilon_0}\cos \alpha_2' \qquad (3.3.17)$$

$x$ = distance between the upper wall and the observer

$d$ = distance between the upper wall and the source

$H$ = distance between the upper wall and the air-dielectric interface.

$h$ = width of the dielectric layer

The inner series may be grouped and a new term, $\gamma(\alpha')$, introduced:*

$$\gamma(\alpha') = r_1 - t_1 t_2 e^{-2b_2 h} + r_2 t_1 t_2 e^{-4b_2 h} - \ldots$$

$$= \frac{r_1 - e^{-2b_2 h}}{1 - r_1 e^{-2b_2 h}} \qquad (3.3.18)$$

Using the optical matrix method show in Appendix A3.2, $\gamma(\alpha')$ is found to be the plane wave reflection coefficient.

Each ray is scattered in the same manner as the incident ray after one reflection at the upper conducting wall, as shown in Figure (3.2.1), such that the field may be expressed as an infinite series of terms, i.e.

$$\left[e^{-b_1(x-d)} - e^{-b_1(x+d)}\right]\left[1 + e^{-2b_1(H-x)}\gamma(\alpha')\right]$$

$$\cdot\left[1 - \gamma(\alpha') e^{-2b_1 H} + \gamma^2(\alpha') e^{-4b_1 H} - \ldots\right] \qquad (3.3.19)$$

This reduces to a closed form expression for the field on two scattered plane waves, due to the source and one image, at an angle $\alpha'$ as given by:

$$\frac{2 \sinh (b_1 d)\, e^{-b_1 x}\left[1 + \gamma(\alpha') e^{-2b_1(H-x)}\right]}{\left[1 + (\alpha') e^{-2b_1 H}\right]} \qquad (3.3.20)$$

---

* For complete derivation of equation (3.3.18) see Appendix (A3.8).

The denominator of (3.3.20) is the right hand side of the characteristic equation. A solution is possible when the denominator equals zero, i.e.:

$$1 + \gamma(\alpha')e^{-2b_1 H} = 0 \qquad (3.3.21)$$

This can be reduced to the well-known transverse impedance matching equation[12] given by:

$$\beta_1 \tan(\beta_2 h)\cos(\beta_1 H) + \beta_2 \sin(\beta_1 H) = 0 \qquad (3.3.22)$$

where the following are defined as:

$$\beta_1 = b_1/i$$

$$\beta_2 = b_2/i$$

At this point, the exact solution may be found by first reducing the integrand, (3.3.20), to the form:

$$\frac{2\sinh(b_1 d)[\beta_1 \tan(\beta_2 h)\cos(\beta_1(H-x)) + \beta_2 \sin(\beta_1(H-x))]}{\beta_1 \tan(\beta_2 h)\cos(\beta_1 H) + \beta_2 \sin(\beta_1 H)} \qquad (3.3.23)$$

and then applying the residue theory to get the $LSE_{mo}$ mode solution, i.e.:

$$E_y = -\omega\mu I_o \sum_{m=1}^{\infty} \frac{(1/\$)\sin(\beta_1 x).\sin(\beta_1 d)\, e^{j\$z}}{H + D^2 h - \left[\frac{\sin(2\beta_1 H)}{2\beta_1} + \frac{D^2\sin(2\beta_2 h)}{2\beta_2}\right]} \qquad (3.3.24)$$

where D is defined as follows:

$$D = \frac{\sin(\beta_1 H)}{\sin(\beta_2 h)} \qquad (3.3.25)$$

This is the exact form derived in Section 3.4 using $LSE_{mo}$ modes and the integral equation method.

3.3.3 Approximate Solution of the Single Layer Case

The approximate solution is based on the characteristic equation expanded as a sum of ray fields, i.e.:

$$e^{i2\beta_1 H} + \left[ r_1 - t_1 t_2 e^{-i2\beta_2 h} + r_2 t_1 t_2 e^{-i4\beta_2 h} - \ldots \right] = 0 \quad (3.3.26)$$

If the coefficients $\beta_1$ and $\beta_2$ are real, rays propagate in the guide at angles $\alpha$ and $\beta$ (measured with respect to the normal of the air-dielectric interface) subject to the eigenvalue solution of (3.3.26).

Equation (3.3.26) may be approximated if the reflection coefficient $r_1$ is small by the simple form:

$$e^{i2\beta_1 H} - e^{-i2\beta_2 h} = 0 \quad (3.3.27)$$

which implies that:

$$(\beta_1 H + \beta_2 h) = \pi L \quad (3.3.28)$$

where L is an integer greater than zero. Since the relation between $\beta_1$ and $\beta_2$ is well known, i.e.,

$$\beta_2^2 - \beta_1^2 = K^2(\varepsilon/\varepsilon_o - 1) \quad (3.3.29)$$

an approximate solution for $\beta_1$ can be found in terms of H,h,$\varepsilon$,K and L by solving the following quadratic equation:

$$\beta_1^2(H^2-h^2) + \beta_1(-2\pi HL) + [(\pi L)^2 - h^2(\varepsilon/\varepsilon_o - 1)K^2] = 0 \quad (3.3.30)$$

The solution of (3.3.30) is a valid linear approximation only for certain values of $\varepsilon$ as shown in Figure (3.3.2), that is, when a surface wave is not

EIGENVALUE SOLUTION OF THE RECTANGULAR GUIDE LOADED BY A SINGLE DIELECTRIC LAYER

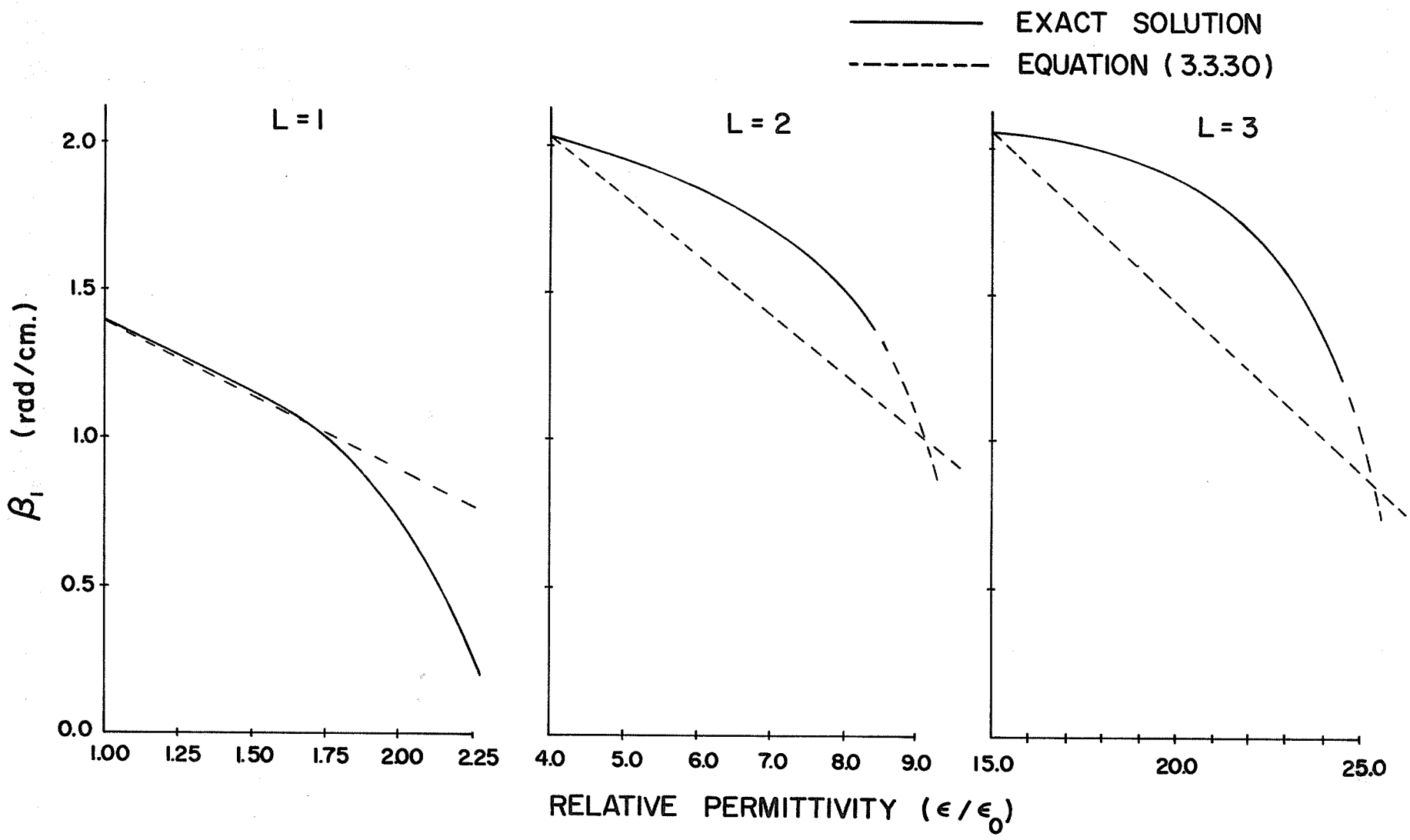


FIGURE (3.3.2)

the dominant propagating mode in the waveguide. Thus we can predict the type of mode structure as a function of $\varepsilon$ by examining the solution of (3.3.30) when L is an integer and $\beta_1$ lies in the range $0<\beta_1<K$.

As shown by the numerical example in Section 3.3.4, the accuracy of the approximation is improved by accounting for more rays, that is, by including reflected rays. However, this method of reducing the error has definite computational limitations. Figure (3.3.3) shows a graphical representation of the plane wave reflection coefficient for various values of permittivity $\varepsilon$.* It is apparent that the magnitude of the reflection coefficient increases to unity with increasing permittivity and becomes complex as $\varepsilon$ is increased further. Consequently, since the magnitude of $r_1$ can equal unity, the closed form of the summation rather than the approximation may be needed.

The complex reflection coefficient can be explained by considering the basic limitations of this coefficient. It can be inferred from Figure (3.3.3) that the magnitude of the reflection coefficient cannot exceed unity.** Recalling that $r_1$ is defined by the expression:

$$r_1 = \frac{\beta_1 - \beta_2}{\beta_1 + \beta_2} \qquad (3.3.31)$$

and that $\beta_2$ and $\beta_1$ are related by the following:

$$\beta_2^2 - \beta_1^2 = K^2(\varepsilon/\varepsilon_o - 1) \qquad (3.3.32)$$

It is evident that the difference between $\beta_2$ and $\beta_1$ must increase with increasing $\varepsilon$, if K is a constant, and hence $r_1$ must increase. However, since the magnitude of $r_1$ cannot exceed unity, (3.3.32) can be justified if $\beta_1$ and $r_1$ are allowed to become complex.

---

* $r_1$ is based on (2.5.1) and the exact solution.

** This is assumed to be valid for the field scattered by a dielectric layer.

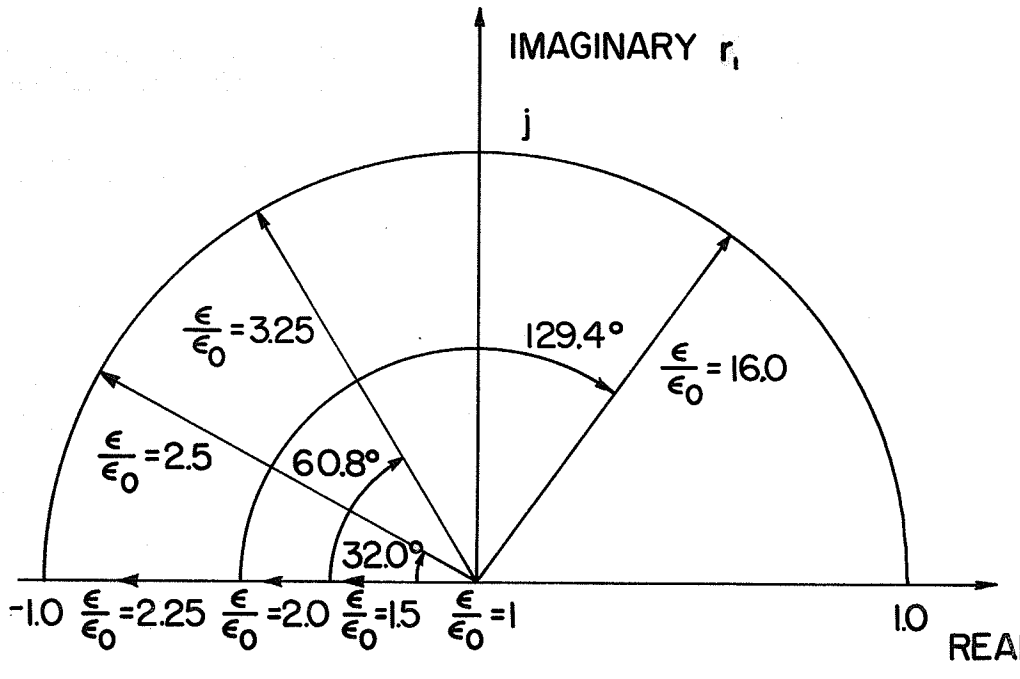


GRAPHICAL REPRESENTATION OF THE PLANE WAVE REFLECTION COEFFICIENT AS A FUNCTION OF LAYER PERMITTIVITY CORRESPONDING TO THE FIRST PROPAGATING MODE

FIGURE ( 3.3.3 )

Wave propagation for the case when $r_1$ is complex may be interpreted using diffracted rays. The complex coefficients result if it is assumed that rays propagate in the loaded region and are incident on the air-dielectric interface at an angle greater than the critical. Hence total reflection occurs for these rays while a diffracted field in the form of a surface wave propagates in the unloaded region. This interpretation is similar to interpretations made by other authors for problems involving surface wave propagation[17].

Thus an approximate solution has been developed for the case when both $\beta_1$ and $\beta_2$ are real. This approximation is not useful if $r_1$ is large (approximately unity) since a large number of rays must be analysed and the fields on these rays summed. For this case it is more convenient to use the closed form of the characteristic equation.

### 3.3.4 Approximate Solution of the Multi-Layer Case

The method of Section (3.3.3) is extended to the multi-layer case with particular emphasis on four dielectric layers.

It follows from the previous section that the characteristic equation for a guide containing an arbitrary number of layers, N, can be found by expressing $\gamma(\alpha')$ as an infinite series of ray fields. Thus if all eigenvalues are real, an approximate solution may be obtained by summing only a finite number of ray fields to satisfy (3.3.21).

$\gamma(\alpha')$ is derived in Appendix A3.3 for the two layer case in terms of an infinite series of ray fields. If the reflection coefficients are small ($r_i^2 \sim o$), this reduces to a simple expression given by:

$$\gamma(\alpha') = r_1 + r_2 e^{-i2} \, 1_{-e}^{-i2(\xi_1+\xi_2)} \quad -r_2 e^{-i2(\xi_1+2\xi_2)} \quad -r_1 e^{-i4(\xi_1+\xi_2)} \qquad (3.3.33)$$

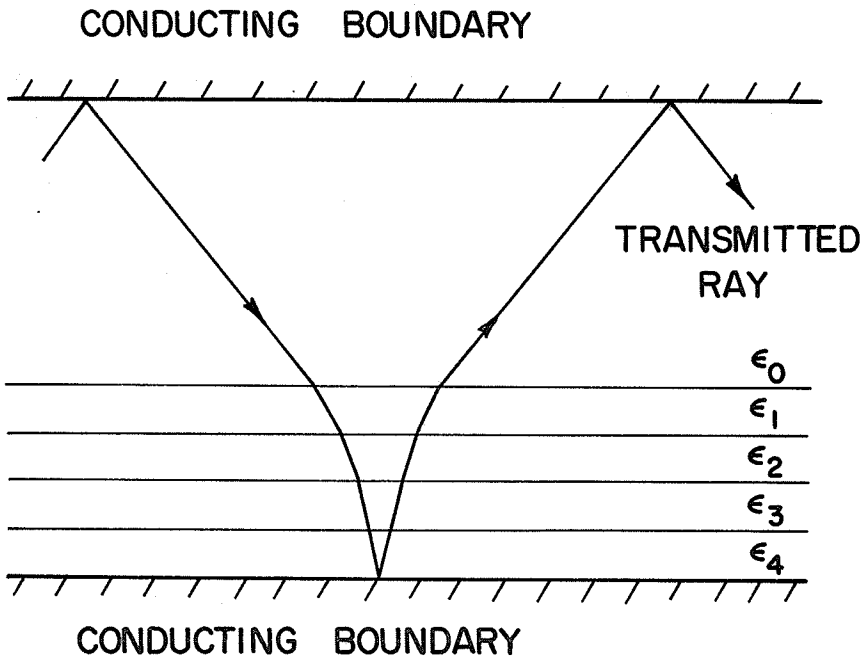


PATH OF THE TRANSMITTED RAY FOR THE FOUR LAYER CASE

FIGURE (3.3.4)

EIGENVALUE SOLUTION OF THE RECTANGULAR GUIDE LOADED BY FOUR DIELECTRIC LAYERS

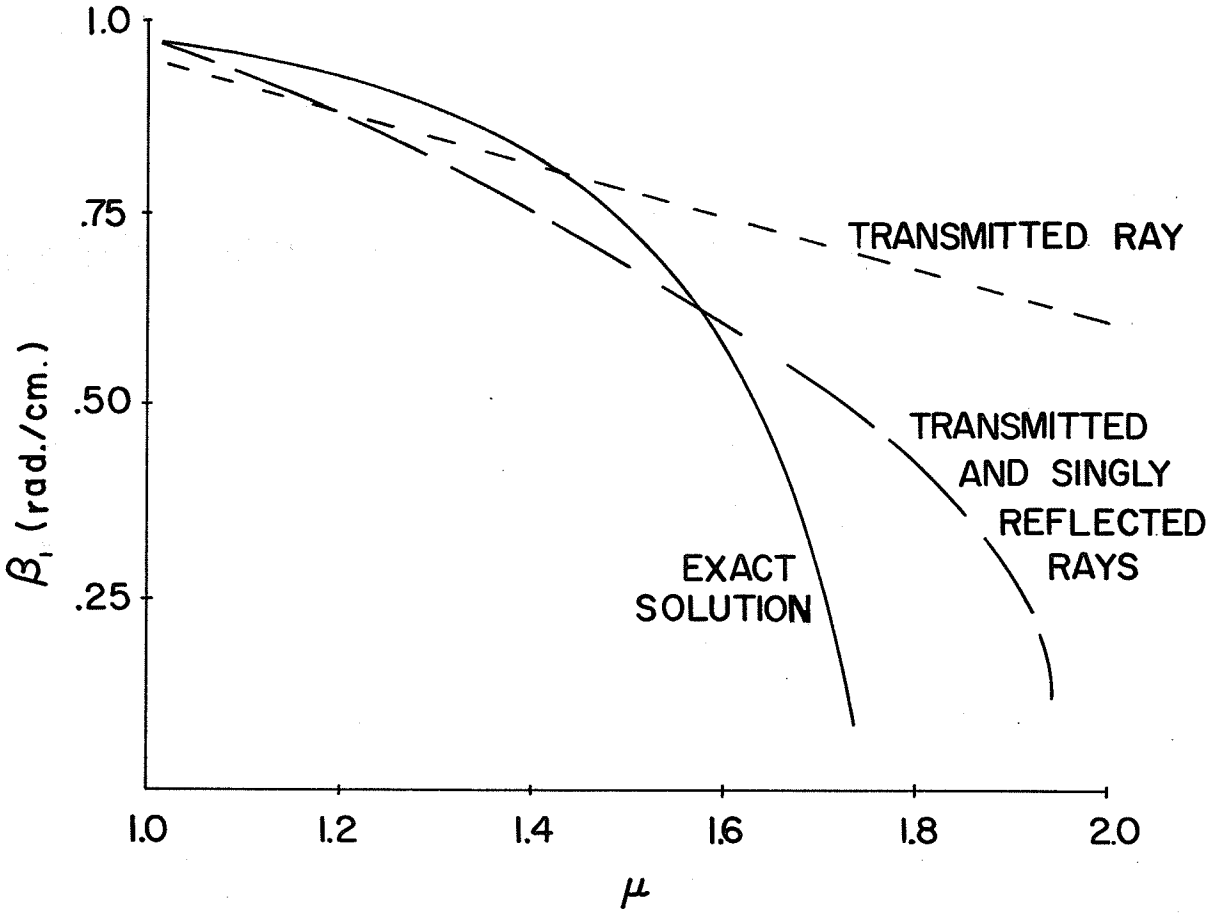


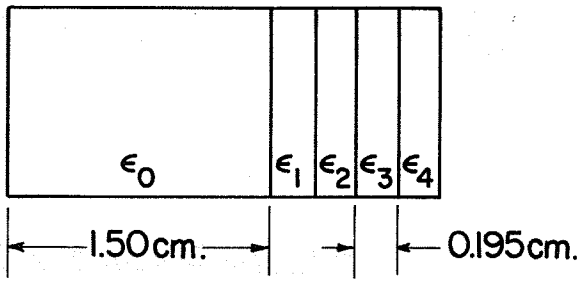


$$\epsilon_1 = \epsilon_0(1 + .375\mu)$$
$$\epsilon_2 = \epsilon_0(1 + .750\mu)$$
$$\epsilon_3 = \epsilon_0(1 + 1.125\mu)$$
$$\epsilon_4 = \epsilon_0(1 + 1.500\mu)$$

FIGURE (3.3.5)

For the four layer case $\gamma(\alpha')$ may be expressed by one transmitted ray and eight reflected rays or simply by one transmitted ray if $r_i$ is small, where i is the integer: i = 1,2,3,4. Hence for N layers, $\gamma(\alpha')$ may be expressed by one transmitted ray and 2N reflected rays if $r_i^2$ is small or simply by one transmitted ray if $r_i$ is small, where i is the integer: 1,2,3...,N. The transmitted ray for the four layer case is shown in Figure (3.3.4). The solution for the four layer case using only the transmitted ray is compared to the exact solution in Fig. (3.3.5). In addition, a solution based on the transmitted ray and eight reflected rays is compared to the exact solution.

## 3.4 Comparison with the Exact Solution for an Arbitrary Number of Layers

The exact solution previously used to check the approximate results of Sections (3.2) and (3.3) is discussed.

The electric and magnetic fields are completely expressed in terms of $LSE_{mo}$ (longtitudinal section electric) modes when a line source,* parallel to the short dimension of the guide, excites a field in the transversely loaded guide[11,12]. The electric field for an N layer guide has the following form:

$$E(x,o) = \begin{cases} \sum_{m=1}^{\infty} A_{1m} \sin \beta_{1m} x & o<x<x_1 \\ \sum_{m=1}^{\infty} (A_{2m} \sin\beta_{2m} x + A'_{2m} \cos\beta_{2m} x) & x_1<x<x_2 \\ \sum_{m=1}^{\infty} A_{(N+1)m} \sin\beta_{(N+1)m} x & x_{N-1}<x<a \end{cases} \qquad (3.4.1)$$

---

* $TE_{mo}$ for empty guide.

where the axial dependence is understood to be of the form:

$$e^{j\xi_m Z} \tag{3.4.2}$$

The magnetic field is expressed in a similar form as given in Appendix A3.4.

The unknown coefficients are found by matching the electric and magnetic fields at each dielectric interface: $x_1, x_2, \ldots, x_N$. Since both electric and magnetic fields are matched at N interfaces, for the N layer case, there will be 2N independent equations in terms of the following unknowns:

$$A_1, A_2, \ldots, A_N, A_{N+1}$$
$$A_2', \ldots, A_N'$$
$$\beta_1, \beta_2, \ldots, \beta_N, \beta_{N+1}$$

The equations may be represented in a 2N x 2N matrix in terms of $A_1, A_2, A_2', \ldots$ whose determinant vanishes. Using equation (3.3.29) in the general representation, the determinant may be solved to find $\beta_1, \beta_2, \ldots, \beta_{N+1}$. Once these coefficients are obtained, the remaining coefficients may be determined in terms of $A_1$ by matrix inversion.

The amplitude coefficients are found by evaluating $A_1$ for the case of line source excitation. A current line source is at the point $(x_o, 0)$ and is of the form:

$$\bar{J} = I_o \hat{i}_y \delta(x-x_o)\, \delta(Z) \tag{3.4.3}$$

The reciprocity theorem in a reduced form is applied to solve for the mode coefficients, i.e.:

$$\iint_S (\bar{E}^a \times \bar{H}^b - \bar{E}^b \times \bar{H}^a).d\bar{s} = -\iiint_V \bar{E}^a . \bar{J}^b \, dv \tag{3.4.4}$$

Following the steps outlined in Appendix A3.5, the coefficient $A_{1n}$ is found for the two layer guide:

$$A_{1n} = \frac{-I_o \omega \mu (1/K_z) \sin \beta_1 X_o . e^{jK_z (Z-Z_o)}}{x_1 + D^2(a-x_1) - \left[ \frac{\sin (2\beta_1 X_1)}{2\beta_1} + D^2 \frac{\sin (2\beta_2 (a-X_1))}{2\beta_2} \right]} \qquad (3.4.5)$$

The denominator can be extended to N + 1 integrals for N layers, i.e.:

$$2\int_0^{x_1} \sin^2\beta_1 x . dx + 2\int_{x_1}^{x_2} \left(\frac{A_2}{A_1}\sin\beta_2 x + \frac{A_2}{A_1}\cos\beta_2 x\right)^2 dx + \ldots + 2\int_x^a A_{N+1}{}^2 \sin(\beta_1(a-x))dx \qquad (3.4.6)$$

It is now clear that the following three steps are followed in order to find the $LSE_{mo}$ mode solution using the integral equation method:

1) solve the 2N x 2N determinant for $\beta_1, \beta_2, \ldots$
2) invert the (2N-1) x (2N-1) matrix to find $A_2/A_1$, $A_2'/A_1, \ldots$
3) solve N + 1 integrals

Appendix A3.6 presents a solution of the single layer case for twenty-four values of layer permittivity. In addition, the 8 x 8 matrix for the four layer guide is presented in Appendix A3.7. Standard computer techniques were used to find these numerical solutions[17,18].

The exact and approximate solutions are compared graphically in Figures (3.2.3), (3.2.4), (3.3.2) and (3.3.5). The first two figures show the electric field of the propagating $LSE_{10}$ mode compared to the finite summation of ray fields. Figure (3.2.2) shows a plot of the eigenfunction $\beta_1$ for various ranges of layer permittivity while Figure (3.3.5) shows $\beta_1$ for

the four layer case for certain values of $\varepsilon_1, \varepsilon_2, \varepsilon_3$ and $\varepsilon_4$. In each case, the exact and one of the approximate solutions are compared.

# CHAPTER IV

## CONCLUSIONS AND SUGGESTIONS FOR FUTURE RESEARCH

### 4.1 Conclusions

The derivations and results presented in the previous chapters permit certain conclusions with regard to the effectiveness of these methods and physical interpretations of the reflection coefficient and surface wave propagation.

Examination of the results based on the asymptotic ray technique show that the approximations are valid for the rays shown in Figure (3.2.2) and equations (2.3.3) and (A2.2.5) describing the fields on these rays. The technique leads to the graphical results shown in Figures (3.2.3) and (3.2.4) and indicates reasonable accuracy when the significant ray fields are summed. Thus for the particular cases of $\varepsilon = 1.5\varepsilon_o$ and $\varepsilon = 2.0\varepsilon_o$ the errors in the amplitude and phase, based on these significant rays, are small. For both cases, error in the amplitude is less than 5% as shown in Figure (3.2.3), while the phase error is less than 5° for an electrical path length of 720° between the source and the observer.* However, it is apparent from Figure (3.2.4) that the errors increase with increasing permittivity due to the higher order reflected rays being neglected in the summation.** Since Figure (3.2.4) is based on all possible rays except those reflected at the air-dielectric interface, it is apparent that the accuracy of the method may be improved by taking the neglected rays into account. The results would still not be exact until the higher order terms of (2.3.3) are taken into account. Thus for the single layer case the ray method is simple and has certain attractive features provided an

---

* Calculated from Appendix A3.1.

** See Appendix A3.1.

approximate solution based on the most significant rays is desired. For improved accuracy, the summation of neglected rays requires further numerical techniques to classify the rays and describe their field amplitude and phase.

For the case of multiple dielectric layers loading the waveguide, the angular spectrum of plane waves technique is formally developed in Section (3.3). The accuracy of the resulting expresions depends on the characteristic equation (3.3.21). For the cases where the permittivity of adjacent layers is approximately equal, the approximation for $\gamma(\alpha')$ as developed in Appendix A3.3 is of a limited use as shown by the solutions in Figures (3.3.2) and (3.3.5). However, the accuracy of the results depends on the number of terms taken in (A3.3.3). Figure (3.3.5) shows a large error for the four layer case when only the first term due to the transmitted ray is taken into account. It is expected therefore that the accuracy of the method will improve provided that a computational technique is developed to account for the large number of higher order rays. Similarly as the interlayer reflection coefficient increases, the accuracy of the two term approximation deteriorates since the effect of the higher order reflected rays becomes more pronounced. For all such cases, the determinant for the exact solution (see A3.7) should be evaluated rather than summing a large number of ray fields.

For particular solutions of the characteristic equation, complex values for the reflection coefficient were found as discussed in Section (3.3.3), and an interpretation is made in terms of diffracted rays as encountered in similar problems[3,6,17]. Thus the solution of the characteristic equation for the single layer case may result in an imaginary $\beta_1$ such that the electric field varies as $\sinh(b_1 x)$ in the unloaded region (1)

shown in Figure (A3.6). Furthermore if $\beta_2$ is real, plane waves propagate in region (2) exciting a diffracted field in region (1) if the plane waves are incident on the air-dielectric interface at an angle greater than the critical angle. For the case of a single dielectric layer of finite thickness and infinite length inserted in the waveguide, as shown in Figure (4.2.1a), the field solution may consist of imaginary eigenvalues in the unloaded regions and a real eigenvalue solution in the loading layer. Physically, this corresponds to plane waves propagating in the layer and surface waves due to diffracted rays in the unloaded regions. Thus, whenever the solution of the characteristic equation results in a complex reflection coefficient, a physical interpretation in terms of plane wave rays and diffracted rays may be made.

## 4.2 Suggestions for Future Research

It is apparent from the conclusions that the development of numerical methods and logic schemes could possibly be a valuable aid in the summation of reflected rays appearing in the asymptotic solution. This appears to be difficult at present but if developed would make the ray method a much more powerful tool for the numerical solution of waveguide problems involving inhomogeneous anisotropic layers.

The phase shifter shown in Figure (4.2.1a) is one specific problem that may be solved using the ray-optical technique.* Since the total number of significant rays in this case is considerably larger than the single layer of Section (3.2), a numerical program could be made to determine phase shift versus transverse position of the slab. The resulting numerical solution could be useful for predicting the behaviour and phase shift of similar devices where the slab may not be lossless, homogeneous and isotropic.

---

* Corner diffracted rays must be included.

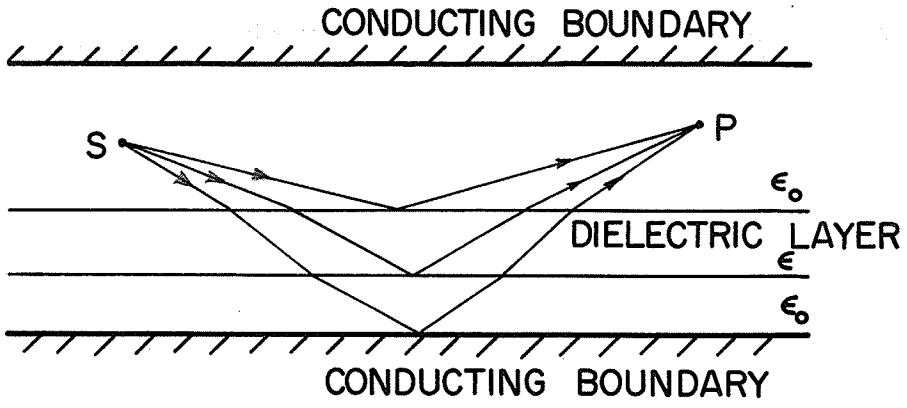


(a) PHASE SHIFTER

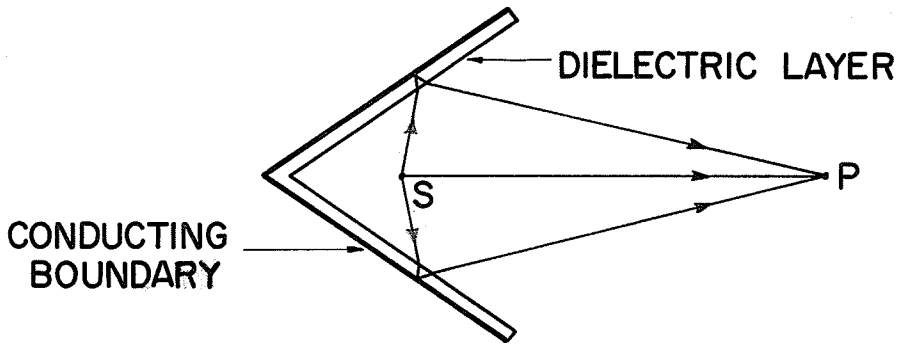


(b) DIELECTRIC-LOADED CORNER REFLECTOR

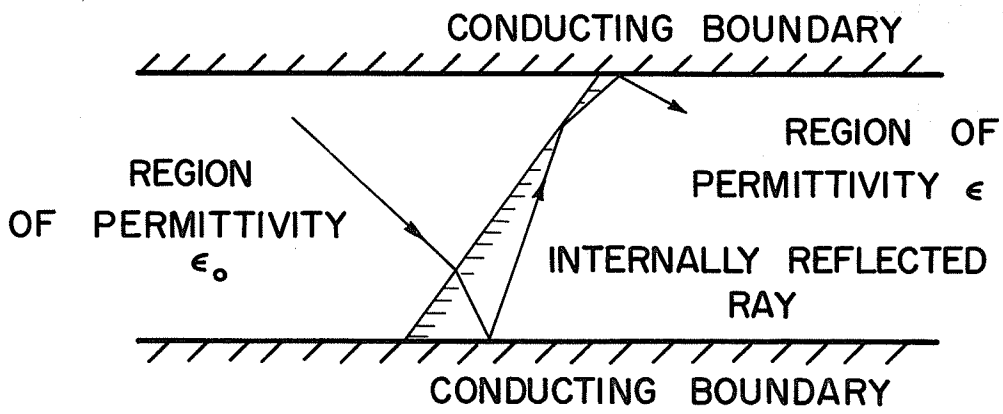


(c) H - PLANE WEDGE

FUTURE RESEARCH PROBLEMS

FIGURE (4.2.1)

The ray method could be especially useful when applied to radiation problems such as in the cases of the dielectric-loaded corner reflector or the E and H-flared horn. Using very simple principles and without any previous knowledge of the final form of the field, beam focussing by these devices could be found using ray theory. The final form of the field may be found in terms of geometrical and diffracted rays. Geometric rays would be traced from a source within the horn or reflector to the observation point as shown in Figure (4.2.16). The diffracted rays from the operture are then added to the geometrical optics solution to obtain the final value of the field. Radiation problems, such as these, are especially suited to the ray method since only a few rays need be summed while alternate methods, such as the boundary value method, are difficult to solve.

Further research should be done for certain problems where a diffracted field is excited by propagating plane wave incident on an air-dielectric boundary, at an angle greater than critical.

As an example of such a problem, consider the case of an H-plane dielectric wedge loading a rectangular guide as shown in Figure (4.2.1C). Here the scattering coefficients have been attempted both experimentally and numerically by the author and now certain conclusions are apparent. The numerical solution consisted of tracing and summing a finite number of scattered rays. These rays are traced from two incident plane waves corresponding to an incident $TE_{10}$ mode. The ray solution has been found to be very accurate when rays were not totally internally reflected. However, when total internal reflection occurred, the field could not be summed because of the diffracted surface waves.* Even though these results are not complete, it is apparent that the ray theory can be extremely use-

---

* These are difficult to sum.

ful for certain problems where the eigenfunction solution cannot be used but a ray solution may be found by summing only a few rays.

# BIBLIOGRAPHY


1. Seckelmann, R., "Propagation of TE Modes in Dielectric Loaded Waveguides", IEEE Transactions on Microwave Theory and Techniques, Vol. MTT-14, No. 11, Nov. 1966, pp. 518-527.

2. Eberhardt, N., "Propagation in the Off Centre E-Plane Dielectrically Loaded Waveguide", IEEE Transactions on Microwave Theory and Techniques, Vol. MTT-15, No. 5, May 1967, pp. 282-289.

3. Keller, J.B., Lewis, R.M., and Seckler, B.D., "Asymptotic Solution of Some Diffraction Problems", Communications on Pure and Applied Mathematics, Vol. 9, No. 2, May 1956, pp. 207-265.

4. Booker, H.G., and Clemmow, P.C., "The Concept of Angular Spectrum of Plane Waves, and the Relations to that of Polar Diagram and Aperture Distribution", Journal of the IEE, Vol. 97, Part 3, Paper No. 922R, January 1950, pp. 11-17.

5. Officer, C.B., "Normal Mode Propagation in a Three Layer Liquid Half-Space by Ray Theory", Geophysics, Vol. 16, 1951, pp. 207-212.

6. Born, M., and Wolf, E., Principles of Optics, third edition, Pergamon Press, London, 1965.

7. Sommerfeld, A., and Runge, J., "Anwendung der Vektorrechung auf die Grundlagen der Geometrischen Optik," Annalen Der Physik, Vol. 35, 1901, pp. 277-298.

8. Silver, S., Microwave Antenna Theory and Design, MIT Radiation Laboratory Series, Vol. 12, McGraw-Hill, 1949.

9. Keller, J.B., "Diffraction by a Convex Cylinder", Electromagnetic Wave Theory Symposium, IRE Transactions on Antennas and Propagation, Vol. AP-4, No. 7, July 1956, pp. 312-321.

10. Keller, J.B. and Friedricks, K.O., "Geometrical Acoustics II, Diffraction, Reflection and Refraction of a Weak Spherical or Cylindrical Shock at a Plane Interface", Journal of Applied Physics, Vol. 26, No. 8, August 1955, pp. 961-966.

11. Collin, R.F., Field Theory of Guided Waves, McGraw-Hill, 1960.

12. Harrington, R.F., Time-Harmonic Electromagnetic Fields, McGraw-Hill, 1961.

13. Pekeris, C., "Theory of Propagation of Explosive Sound in Shallow Water", The Geological Society of America, Memoir 27, Oct. 15, 1948.

14. Brekhovskikh, L.M., Waves in Layered Media, translated from the Russian by D. Liebermann, Academic Press, London, 1960.

15. Morse, P., and Feshback, H. Methods of Theoretical Physics, McGraw-Hill, 1953, part I.

16. Kreyszig, E., Advanced Engineering Mathematics, John Wiley and Sons, Inc., 1962.

17. Adler, R., Chu, L., and Fano, R., Electromagnetic Energy Transmission and Radiation, John Wiley and Sons, Inc., 1960.

18. McCracken, D.D., A Guide to Fortran IV Programming, John Wiley and Sons, Inc., New York 1965.

19. McCormick, J.M., and Salvadori, M.G., Numerical Methods in Fortran, Prentice Hall, Inc., 1961.

APPENDIX A2.1

## DERIVATION OF D(X,Y) AND E(X,Y)

The coefficients D(x,y) and E(x,y) for the rays shown in Figure (2.4.2) are evaluated by matching fields across the plane air-dielectric interface. This is an extension of Keller's solution used to evaluate B(x,y) and C(x,y)[3].

The ray fields may be represented in the following form:

$$\psi = \frac{e^{iK'\phi}}{\sqrt{iK'}} C(x,y) + \frac{e^{iK'\phi}}{\sqrt{iK'}} D(x,y) \qquad \text{(A2.1.1)}$$

and

$$\psi = \frac{e^{iK\eta}}{\sqrt{iK}} E(x,y) \qquad \text{(A2.1.2)}$$

where C,D, and E, are shown in Figure (2.4.2). The boundary conditions, given by equations (2.4.1) and (2.4.2), are applicable at the air-dielectric interface. From these equations, two useful relations may be derived, i.e.:

$$a(iK')^{-1/2} C(x,y) + a(iK')^{-1/2} D(x,y) = (iK)^{-1/2} E(x,y) \qquad \text{(A2.1.3)}$$

and

$$b \frac{\partial\phi}{\partial y} (iK')^{1/2} C(x,y) + b \frac{\partial\phi}{\partial y} (iK')^{1/2} D(x,y) = \frac{\partial\eta}{\partial y} (iK)^{1/2} E(x,y) \qquad \text{(A2.1.4)}$$

where $y = -c$ and x is fixed by $\alpha$ and h. Solving these equations, D(x,y) and E(x,y) are found at the plane interface ($y = -c$) to be of the form:

$$D(x,-c) = C(x,-c) \left( \frac{\frac{\partial \eta}{\partial y} - \frac{b\mu}{a} \frac{\partial \phi}{\partial y}}{\frac{\mu b}{a} \frac{\partial \phi}{\partial y} + \frac{\partial \eta}{\partial y}} \right)$$

$$= C(x,-c) \quad \frac{V - 1}{V + 1} \qquad \text{(A2.1.5)}$$

$$\text{and } E(x,-c) = C(x,-c)\, a\mu^{-1/2} \frac{2V}{1 + V} \qquad \text{(A2.1.6)}$$

It may be deduced from (A2.1.5) and (A2.1.6) that the ray field intensity can be solved using the plane wave reflection and transmission coefficients, given by equations (2.5.1) and (2.5.2), combined with the incremental analysis since the waves are scattered as plane waves at the interface.

# APPENDIX A2.2

## DERIVATION OF FIELD INTENSITY USING INCREMENTAL ANALYSIS

The field intensity on a ray may be found using plane-wave reflection coefficients and an incremental analysis.

C(x,y) is found by matching fields across the first air-dielectric interface of Figure (2.4.2) or using the incremental analysis method. This latter method is based on the application of equation (2.2.3) using an "incremental diagram". From the incremental analysis, C(x,y) may be written directly in the form:

$$\frac{2}{1 + V} \; (h \sec\alpha)^{-1/2} \; \left(\frac{\Delta\ell_2}{\Delta\ell_3}\right)^{1/2} \qquad \text{(A2.2.1)}$$

where the ratio of incremental lengths is written as follows:

$$\left(\frac{\Delta\ell_2}{\Delta\ell_3}\right)^{1/2} = \frac{h \sec^2\alpha.\cos\beta}{(\sin\beta)^{-1}} \; \frac{1}{h\mu^{-1}\frac{\tan\alpha\cos\beta}{\cos\alpha} + \frac{(x-h)\tan\alpha}{\sin\beta} \; \mu^{-2}\frac{\sin\alpha.\cos\alpha}{\cos\beta}}$$

(A2.2.2)

Using (A2.2.2), (A2.2.1) reduces to Keller's form for C(x,y) given by equation (2.4.7).

In a manner similar to the solution of C(x,y), higher order ray fields may be easily evaluated. Consider a finite number of plane parallel finite dielectric layers spaced distances $S_1$, $S_2$,...,$S_n$ apart and of widths $w_1$, $w_2$,..., $w_{n+1}$. Intensity of the field on a ray transmitted through a single layer is as follows:

$$|\psi(x,y)| = \frac{2V}{(1+V)^2} (h \sec \alpha)^{-1/2} \left[ 1 + \frac{w_1 \cos^3\alpha}{\mu h \cos^3\beta} \right]^{-1/2}$$

$$\cdot \left[ 1 + \frac{|y + w_1|}{h + \frac{w_1}{\mu} \sec^3\beta \cos^3\alpha} \right]^{-1/2} \qquad \text{(A2.2.3)}$$

or for two layers it is of the form:

$$|\psi(x,y)| = \left[ \frac{2V}{(1+V)^2} \right]^2 (h \sec \alpha)^{-1/2}$$

$$\cdot \left[ 1 + \frac{w_1 \cos^3\alpha}{\mu h \cos^3\beta} \right]^{-1/2} \left[ 1 + \frac{w_2 \cos^3\alpha}{\mu h \cos^3\beta + w_1 \cos^3} \right]^{-1/2}$$

$$\cdot \left[ 1 + \frac{S_1}{h + \frac{w_1}{\mu} \sec^3\beta \cos^3\alpha} \right]^{-1/2} \left[ 1 + \frac{|y + w_1 + w_2 + S_1|}{h + S_1 + \frac{w_1 + w_2}{\mu} \sec^3\beta . \cos^3\alpha} \right]^{-1/2}$$

(A2.2.4)

(A2.2.4) may be expanded to the case of $n + 1$ layers separated by n spaces. Approximating (A2.2.4), a simple form may be found, i.e.:

$$|\psi(x,y)| = \left( \frac{2V}{(1+V)^2} \right)^{n+1} \left[ \sec \alpha \left\{ h + S_1 + \ldots + S_n + \frac{w_1 + \ldots + w_{n+1}}{\mu} + \Delta y \right\} \right]^{-1/2}$$

(A2.2.5)

where $\Delta y$ is the distance from the last interface to the observer.

Reflected rays are treated in a similar fashion.

## APPROXIMATION FOR THE TRANSMITTED RAYS

This approximation is studied to find the error introduced when (A2.2.5) is used rather than (A2.2.3). Consider the following parameters for the equations:

$h = 1$ cm

$w_1 = 2$ cm

$\Delta y = 1$ cm

$x = 5$ cm

$\mu = 2$

$a = 1$

$b = 1$

The angles $\alpha$ and $\beta$ may be evaluated exactly, i.e.:

$\alpha = 66.0°$

$\beta = 27.2°$

and $V = 4.4$

The results are tabulated as follows:

| Equation | $\lvert\psi\rvert$ |
|---|---|
| (A2.2.3) | 0.23 |
| (A2.2.5) | 0.24 |

It is evident that (A2.2.5) is a good approximation of (A2.2.3) if $\mu$ is not very large compound to unity.

# APPENDIX A3.1

## SUMMATION OF (3.2.2) AND (3.2.3)

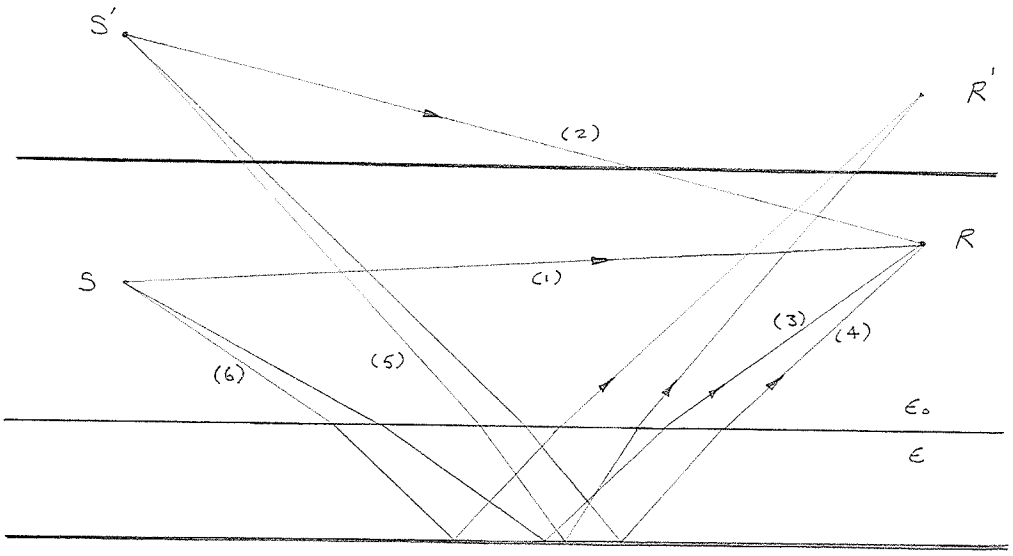


Figure (A3.1)

Six types of rays are summed to give the electric field at the receiver. These are the significant rays if $\varepsilon$ is approximately equal to $\varepsilon_o$,

| | | | |
|---|---|---|---|
| i.e. | (1) | direct | (S-R) |
| | (2) | reflected | (S'-R) |
| | (3) | transmitted | (S-R) |
| | (4) | transmitted | (S'-R) |
| | (5) | transmitted | (S'-R') |
| | (6) | transmitted | (S-R') |

A short computer program is used to sum the fields on types (3), (4), (5) and (6) rays. Equation (A2.2.5) is used rather than the exact form (A2.2.3). The results are tabulated on the following page and plotted on Figures (3.2.3) and (3.2.4).

## ASYMPTOTIC SOLUTION OF THE SINGLE LAYER GUIDE

REFERENCE DISTANCE (cm.)

| PERMITTIVITY | 0.10 | 0.30 | 0.50 | 0.70 | 0.90 | 1.10 |
|---|---|---|---|---|---|---|
| $\varepsilon = 1.5\varepsilon_o$ | | - .044<br>-j.04 | - .070<br>-j.007 | - .093<br>-j.009 | - .109<br>-j.011 | - .124<br>-j.013 |
| $\varepsilon = 2.0\varepsilon_o$ | - .006<br>+j.006 | - .021<br>+j.015 | - .034<br>+j.024 | - .047<br>+j.034 | - .053<br>+j.041 | - .065<br>+j.046 |
| $\varepsilon = 2.5\varepsilon_o$ | | j.017 | .003<br>+j.029 | .003<br>+j.038 | .005<br>+j.048 | .003<br>+j.054 |
| $\varepsilon = 8.0\varepsilon_o$ | | j.035 | j.055 | j.074 | .006<br>+j.085 | j.092 |

## OPTICAL MATRIX METHOD

A well known matrix representation[6] is used to calculate $\gamma(\alpha')$, i.e.:

$$\begin{bmatrix} E^{+}_{m-1} \\ E^{-}_{m-1} \end{bmatrix} = \frac{1}{tm} \begin{bmatrix} e^{i\S m-1} & r_{me}\, i\S m-1 \\ r_{me}\, -i\S m-1 & e^{-i\S m-1} \end{bmatrix} \begin{bmatrix} E^{+}_{m} \\ E^{-}_{m} \end{bmatrix}$$

$$= \frac{1}{tm} \begin{bmatrix} a & b \\ c & d \end{bmatrix} \begin{bmatrix} E^{+}_{m} \\ E^{-}_{m} \end{bmatrix} \qquad \text{(A3.2.1)}$$

where $\gamma(\alpha')$ is defined by the following:

$$\gamma(\alpha') = \frac{c}{a} \qquad \text{(A3.2.2)}$$

rm and tm are the Fresnel coefficients at the plane air-dielectric interface. $E^{+}_{m-1}$, $E^{-}_{m-1}$, $E^{+}_{m}$, $E^{-}_{m}$ are the incident and reflected fields respectively. at the side m-1 and the side m of a finite dielectric layer. This method is used to find $\gamma(\alpha')$ for the single and double layer case.

For the single layer case, the abcd matrix is written as follows:

$$\begin{bmatrix} 1 & r_1 \\ r_1 & 1 \end{bmatrix} \begin{bmatrix} e^{b_2 h} & -e^{-b_2 h} \\ -e^{-b_2 h} & e^{b_2 h} \end{bmatrix}$$

where c/a is of the form:

$$\frac{c}{a} = \frac{r_1 - e^{-2b_2 h}}{1 - r_1 e^{-2b_2 h}}$$

Similarly, the matrix for the two layer case is of the form:

$$\begin{bmatrix} 1 & r_1 \\ r_1 & 1 \end{bmatrix} \begin{bmatrix} e^{b_2 h} & r_2 e^{-b_2 h} \\ r_2 e^{-b_2 h} & e^{b_2 h} \end{bmatrix} \begin{bmatrix} e^{b_3 h'} & -e^{-b_3 h'} \\ -e^{-b_3 h'} & e^{b_3 h'} \end{bmatrix}$$

where c/a is of the form:

$$\frac{c}{a} = \frac{e^{b_3 h'}(r_1 e^{b_2 h} + r_2 e^{-b_2 h}) - e^{b_3 h'}(r_1 r_2 e^{b_2 h} + e^{-b_2 h})}{e^{b_3 h'}(e^{b_2 h} + r_1 r_2 e^{-b_2 h}) - e^{b_3 h'}(r_2 e^{b_2 h} + r_1 e^{-b_2 h})}$$

This matrix method could be extended to evaluate $\gamma(\alpha')$ exactly for N layer.

## RAY INTERPRETATION OF $\gamma(\alpha')$ FOR MULTIPLE LAYERS

Before considering the multi-layer case, the two layer problem is examined in terms of plane waves or rays from a plane wave source.

The reflection coefficient $\gamma(\alpha')$ can be interpreted as done by Officer for the single layer case[5]. The scattered field of a plane wave incident on the second interface can be written as an infinite series of ray fields, i.e.:*

$$\gamma_2(\alpha_2') = r_2 - (1-r_2^2)e^{-i2\xi_2} - r_2(1-r_2^2)e^{-i4\xi_2} - \ldots \quad (A3.3.1)$$

Similary the scattered field of a plane wave incident on the first boundary can be written as an infinite series of ray fields, i.e.:

$$\gamma(\alpha_1')= r_1 + (1-r_1^2)\gamma_2(\alpha_2')e^{-i2\xi_1} - r_1(1-r_1^2)\gamma_2^2(\alpha_2')e^{-i4\xi_1} + \ldots \quad (A3.3.2)$$

$\gamma(\alpha_1')$ can be written as an infinite series of ray fields if (A3.3.1) is substituted for $\gamma_2(\alpha_2')$, i.e.:

$$\begin{aligned}\gamma(\alpha_1') &= r_1 + (1-r_1^2)e^{-i2\xi_1}\left[r_2 - (1-r_2^2)e^{-i2\xi_2} - \ldots\right] \\ &\quad -r_1(1-r_1^2)e^{-i4\xi_1}\left[r_2 - (1-r_2^2)e^{-i2\xi_2} - \ldots\right]^2 + \ldots \\ &= r_1 + (1-r_1^2)r_2e^{-i2\xi_1} - (1-r_1^2)(1-r_2^2)e^{-i2(\xi_1+\xi_2)} \\ &\quad - (1-r_1^2)(1-r_2^2)r_2e^{-i2(\xi_1+2\xi_2)} \\ &\quad - (1-r_1^2)(1-r_2^2)r_1e^{-i4(\xi_1+\xi_2)} - \ldots \qquad (A3.3.3)\end{aligned}$$

The first five ray fields of (A3.3.3) are due to rays singly reflected, refracted, or combined singly reflected refracted. A finite summation that

---

* $r_1$ and $r_2$ are the reflection coefficients at the first and second boundaries respectively.

includes only these rays is a good approximation to (A3.3.3) if $r_1^2$ and $r_2^2$ are small. If $r_1$ and $r_2$ are negligible, the series further reduces to the expression $-(1-r_1^2)(1-r_2^2)e^{-i2(\xi_1 + \xi_2)}$. Hence $\gamma(\alpha_1')$ may be approximated for the N layer case by the single transmitted ray or one transmitted ray and 2N reflected rays.

## APPENDIX A3.4

## LSE MODES*

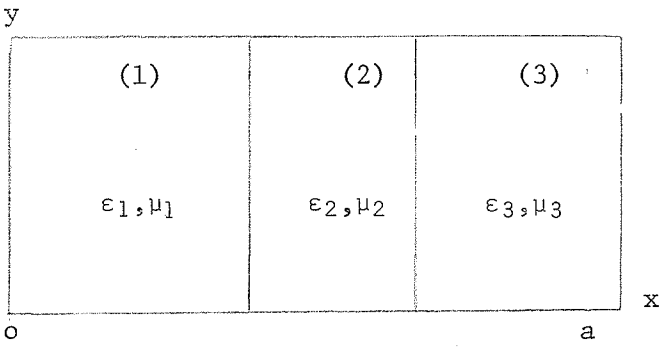


Figure (A3.4)

$$E_{y1} = A_1\omega\mu_1 K_z \sin\beta_1 x$$

$$E_{y2} = A_2\omega\mu_2 K_z (\sin\beta_2 x + A_2'' \cos\beta_2 x)$$

$$E_{y3} = A_3\omega\mu_3 K_z \sin\beta_3 (a-x)$$

$$H_{x1} = -A_1 (K_1^2 - \beta_1^2)\sin\beta_1 x$$

$$H_{x2} = -A_2 (K_2^2 - \beta_2^2)(\sin\beta_2 x + A_2'' \cos\beta_2 x)$$

$$H_{x3} = -A_3 (K_3^2 - \beta_3^2)\sin\beta_3 (a-x)$$

$$H_{z1} = +jA_1\beta_1 K_z \cos\beta_1 x$$

$$H_{z2} = +jA_2\beta_2 K_z (\cos\beta_2 x - A_2'' \sin\beta_2 x)$$

$$H_{z3} = -jA_3\beta_3 K_z \cos\beta_3 (a-x)$$

---

* $LSE_{mo}$ Modes

APPENDIX A3.5

DERVIATION OF (3.4.5)

Proceeding from the Reciprocity Theorem[12], equation (3.4.4) is evaluated by constructing a surface to divide the waveguide into sections A and B at $Z = Z^1$ (B containing the source). Integrating over region A, (3.4.4) is of the following form:

$$\int_0^a \int_0^b (E_y^a H_x^b - E_y^b H_x^a)\, dydx \Big|_{Z=Z^1}^{A} = 0 \qquad (A3.5.1)$$

and similarly (3.4.4) evaluated over B is of the form:

$$+\int_0^a \int_0^b (E_y^a H_x^b - E_y^b E_x^a)\, dydx \Big|_{Z=Z^1}^{B}$$

$$= aI_o\, \omega\mu K_z \sin \beta_1 x_o . e^{-jK_z Z_o} \qquad (A3.5.2)$$

If (A3.5.1) is substituted into (A3.5.2), the following is found:

$$e^{-j2K_z Z} \int_0^a \int_0^b E_y^a H_x^b\, dydx \Big|_{Z=Z^1}^{A} - \int_0^a \int_0^b E_y^a H_x^b\, dydx \Big|_{Z=Z^1}^{B}$$

$$= bI_o\, \omega\mu K_z \sin \beta_1 x_o . e^{-jK_z Z_o} \qquad (A3.5.3)$$

The modes of Appendix (A3.4) are substituted into (A3.5.3), i.e.:

$$\exp(-j2K_z Z) \int_0^c E_y\, (K_1^2 - \beta_1^2) \sin \beta_1 x . \exp(jK_z Z^1)\, dx$$

$$+ \exp(-j2K_z Z) \int_c^a E\, D(K_2^2 - \beta_2^2) \sin \beta_2 (a-x) . \exp(jK_z Z)\, dx$$

$$- \int_{o}^{c} E_y \quad -(K_1^2 - \beta_1^2) \sin \beta_1 x_1 \exp(-jK_z Z^1) \quad dx$$

$$- \int_{c}^{a} E_y \quad -D(K_2^2 - \beta_2^2) \sin \beta_2 (a-x). \exp(-jK_z K_o) \quad dx$$

$$= -I_o \omega\mu K_z \sin \beta_1 x_o. \exp(-jK_z Z_o) \qquad \text{(A3.5.4)}$$

or

$$\int_{o}^{c} E_y (K_1^2 - \beta_1^2) \sin \beta_1 x_1 dx + \int_{c}^{a} E_y (K_2^2 - \beta_2^2) \sin \beta_2 (a-x) dx$$

$$= -I_o \omega\mu K_z \sin \beta_1 x_o \exp\left(jK_z(Z^1 - Z_o)\right) \qquad \text{(A3.5.5)}$$

where $Z_o > Z^1$

For the case $Z^1 > Z_o$, $Z_o$ and $Z^1$ are interchanged.

The field may be satisfied by an infinite sum of $LSE_{mo}$ modes.

$$E_y = \begin{cases} \sum_{m=1}^{\infty} C_m \sin \beta_1 x, & o<x<r \\ \sum_{m=1}^{\infty} C_m^1 \sin \beta_2 x, & c<x<a \end{cases} \qquad \text{(A3.5.6)}$$

$$C_m^1 = C_m D$$

This value of $E_y$ is substituted into (A3.5.5).

Applying orthogonality, a solution for the amplitude coefficient is found, i.e.:

$$C_m = \frac{- I_o \omega \mu (1/K_z) \sin \beta_1 x_o \cdot \exp \quad jK_z(z-z_o)}{2\int_o^c \sin^2 \beta_1 x \cdot dx + D^2\, 2\int_c^a \sin^2 \beta_2 (a-x) dx} \qquad \text{(A3.5.7)}$$

or if the solution is normalized $C_m$ reduces to the following:

$$G = \frac{(1/K_z)}{2\int_o^c \sin^2 \beta_1 x dx + 2\, D^2 \int_c^a \sin^2 \beta_2 (a-x) dx}$$

$$= \frac{(1/K_z)}{c + D^2(a-c) - \left[ \frac{\sin(2\beta_1 c)}{2\beta_1} + D^2 \frac{\sin(2\beta_2 (a-c)}{2\beta_2} \right]} \qquad \text{(A3.5.8)}$$

The equation for G can be generalized to an N layer guide by considering N integrals in the denominator:

$$2\int_o^{x_1} \sin^2 \beta_1 x \, dx$$

$$+ \; 2\int_{x_1}^{x_2} \left( \frac{A_2}{A_1} \sin \beta_2 x + \frac{A_2'}{A_1} \cos \beta_2 x \right)^2 dx$$

$$+ \ldots + 2\int_{x_2}^{a} \left( \frac{An}{A_1} \right)^2 \sin^2 \beta_n (a-x) \, dx$$

## NUMERICAL SOLUTION OF THE SINGLE LAYER CASE*

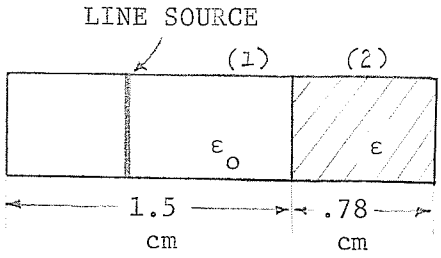


Frequency = 10GHZ,

Figure (A3.6)

### DOMINANT MODES**

| $\varepsilon/\varepsilon_o$ | G | $\beta_1$ | $\beta_2$ | $K_z$ |
|---|---|---|---|---|
| 1.00 | .28 | 1.37 | 1.37 | 1.58 |
| 1.25 | .26 | 1.28 | 1.65 | 1.65 |
| 1.50 | .24 | 1.16 | 1.88 | 1.75 |
| 1.75 | .24 | 0.98 | 2.06 | 1.84 |
| 2.00 | .31 | 0.74 | 2.22 | 1.96 |
| 2.25 | 2.25 | 0.22 | 2.35 | 2.08 |
| 2.50 | j.14 | j.71 | 2.46 | 2.20 |
| 2.75 | j.04 | j1.06 | 2.56 | 2.35 |
| 3.00 | j.015 | j1.34 | 2.64 | 2.48 |
| 3.25 | j.007 | j1.59 | 2.71 | 2.63 |
| 3.50 | j.003 | j1.82 | 2.77 | 2.77 |
| 3.75 | 3.41 | 2.09 | 4.05 | 0.17 |
| 4.00 | 1.48 | 2.06 | 4.17 | 3.93 |
| 5.00 | 0.75 | 1.96 | 4.62 | 0.75 |
| 6.00 | 0.56 | 1.86 | 5.04 | 0.97 |
| 7.00 | 0.43 | 1.73 | 5.41 | 1.17 |
| 8.00 | 0.31 | 1.53 | 5.75 | 1.43 |
| 10.00 | j.13 | 0.78 | 6.24 | 2.23 |
| 16.00 | 1.54 | 2.05 | 8.37 | 4.11 |
| 17.00 | 1.14 | 2.02 | 8.61 | 0.55 |
| 18.00 | 0.92 | 1.99 | 8.86 | 0.66 |
| 20.00 | 0.64 | 1.89 | 9.32 | 0.89 |
| 22.00 | 0.40 | 1.70 | 9.74 | 1.23 |
| 26.00 | j.004 | 1.88 | 10.30 | 2.81 |

---

* Dielectric Layer
** Modes of largest amplitude

APPENDIX A3.7

MATRIX FOR THE FOUR LAYER CASE*

$$
\begin{bmatrix}
\sin(\beta_1 x_1) & -\sin(\beta_2 x_1) & -\cos(\beta_2 x_1) & 0 & 0 & 0 & 0 & 0 \\
\beta_1\cos(\beta_1 x_1) & -\beta_2\cos(\beta_2 x_1) & \beta_2\sin(\beta_2 x_1) & 0 & 0 & 0 & 0 & 0 \\
0 & \sin(\beta_2 x_2) & \cos(\beta_2 x_2) & -\sin(\beta_3 x_2) & -\cos(\beta_3 x_2) & 0 & 0 & 0 \\
0 & \beta_2\cos(\beta_2 x_2) & -\beta_2\sin(\beta_2 x_2) & -\beta_3\cos(\beta_3 x_2) & \beta_3\sin(\beta_3 x_2) & 0 & 0 & 0 \\
0 & 0 & 0 & \sin(\beta_3 x_3) & \cos(\beta_3 x_3) & -\sin(\beta_4 x_3) & -\cos(\beta_4 x_3) & 0 \\
0 & 0 & 0 & \beta_3\cos(\beta_3 x_3) & -\beta_3\sin(\beta_3 x_3) & -\beta_4\cos(\beta_4 x_3) & \beta_4\sin(\beta_4 x_3) & 0 \\
0 & 0 & 0 & 0 & 0 & \sin(\beta_4 x_4) & \cos(\beta_4 x_4) & -\sin(\beta_5(2.28-x_4)) \\
0 & 0 & 0 & 0 & 0 & \beta_4\cos(\beta_4 x_4) & -\beta_4\sin(\beta_4 x_4) & \beta_5\cos(\beta_5(2.28-x_4))
\end{bmatrix}
$$

*Four dielectric layers.

APPENDIX A3.8

DERIVATION OF (3.3.18)

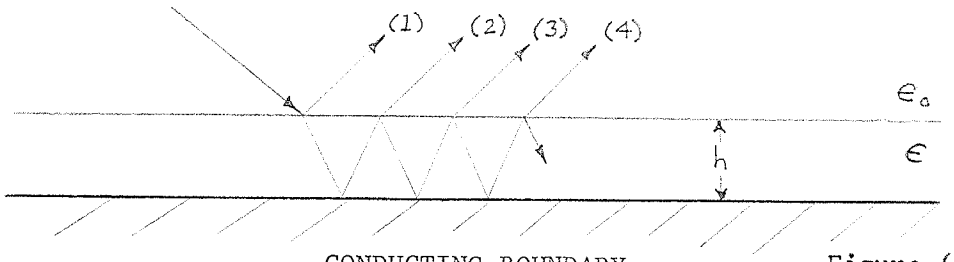


Figure (A3.8)

The field amplitudes on the four types of rays shown in fig. (A3.8) are given by:

(1) $r_1$

(2) $-t_1t_2e^{-2b_2h}$

(3) $t_1t_2r_2e^{-4b_2h}$

(4) $-t_1t_2r_2^2e^{-6b_2h}$

hence:

$$\gamma(\alpha') = r_1 - t_1t_2e^{-2b_2h} + t_1t_2r_2e^{-4b_2h} - t_1t_2r_2^2e^{-6b_2h} + \ldots$$

$$= r_1 - \frac{t_1t_2e^{-2b_2h}}{1 + r_2e^{-2b_2h}}$$

$$= r_1 - \frac{-(1 - r_1^2)\, e^{-2b_2h}}{1 - r_1e^{-2b_2h}}$$

$$= \frac{r_1 - e^{-2b_2h}}{1 - r_1e^{-2b_2h}} \qquad (3.3.18)$$